

C–Cl Oxidative Addition and C–C Reductive Elimination Reactions in the Context of the Rhodium-Promoted Direct Arylation

Laura A. de las Heras, Miguel A. Esteruelas,* Montserrat Oliván, and Enrique Oñate



Cite This: *Organometallics* 2022, 41, 716–732



Read Online

ACCESS |



Metrics & More

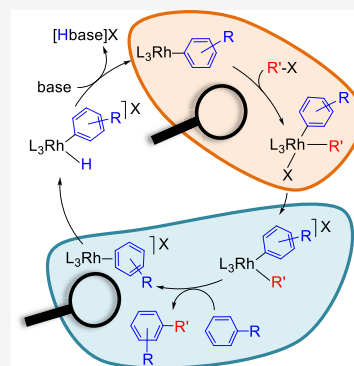


Article Recommendations



Supporting Information

ABSTRACT: A cycle of stoichiometric elemental reactions defining the direct arylation promoted by a redox-pair Rh(I)–Rh(III) is reported. Starting from the rhodium(I)-aryl complex $\text{RhPh}\{\kappa^3\text{-P,O,P-}[\text{xant}(\text{P}^i\text{Pr}_2)_2]\}$ ($\text{xant}(\text{P}^i\text{Pr}_2)_2 = 9,9\text{-dimethyl-4,5-bis-(diisopropylphosphino)xanthene}$), the reactions include C–Cl oxidative addition of organic chlorides, halide abstraction from the resulting six-coordinate rhodium(III) derivatives, C–C reductive coupling between the initial aryl ligand and the added organic group, oxidative addition of a C–H bond of a new arene, and deprotonation of the generated hydride-rhodium(III)-aryl species to form a new rhodium(I)-aryl derivative. In this context, the kinetics of the oxidative additions of 2-chloropyridine, chlorobenzene, benzyl chloride, and dichloromethane to $\text{RhPh}\{\kappa^3\text{-P,O,P-}[\text{xant}(\text{P}^i\text{Pr}_2)_2]\}$ and the C–C reductive eliminations of biphenyl and benzylbenzene from $[\text{RhPh}_2\{\kappa^3\text{-P,O,P-}[\text{xant}(\text{P}^i\text{Pr}_2)_2]\}]\text{BF}_4$ and $[\text{RhPh}(\text{CH}_2\text{Ph})\{\kappa^3\text{-P,O,P-}[\text{xant}(\text{P}^i\text{Pr}_2)_2]\}]\text{BF}_4$, respectively, have been studied. The oxidative additions generally involve the cis addition of the C–Cl bond of the organic chloride to the rhodium(I) complex, being kinetically controlled by the C–Cl bond dissociation energy; the weakest C–Cl bond is faster added. The C–C reductive elimination is kinetically governed by the dissociation energy of the formed bond. The $\text{C}(\text{sp}^3)\text{--C}(\text{sp}^2)$ coupling to give benzylbenzene is faster than the $\text{C}(\text{sp}^2)\text{--C}(\text{sp}^2)$ bond formation to afford biphenyl. In spite of that a most demanding orientation requirement is needed for the $\text{C}(\text{sp}^3)\text{--C}(\text{sp}^2)$ coupling than for the $\text{C}(\text{sp}^2)\text{--C}(\text{sp}^2)$ bond formation, the energetic effort for the pregeneration of the $\text{C}(\text{sp}^3)\text{--C}(\text{sp}^2)$ bond is lower. As a result, the weakest C–C bond is formed faster.

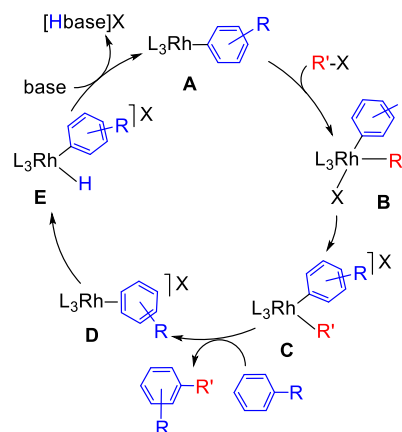


INTRODUCTION

Transition metal-catalyzed C–C cross-coupling reactions are among the industrial technologies of the highest significance.¹ The direct C–H arylation with organic halides is especially appealing among the reactions of this family because it represents a powerful, valuable, and straightforward procedure for nonactivated C–H bond functionalization.² In this context, without a shadow of a doubt, palladium(0) complexes dominate the scene, being the most used catalysts.³ However, examples proving the efficiency of rhodium derivatives have been also reported in recent years,⁴ particularly when alkyl halides are employed.⁵ Three fundamental reactions are the base of the process from the mechanism point of view: the oxidative additions of C–Cl⁶ and C–H⁷ bonds, one of each substrate, to an unsaturated d^n -metal center in low oxidation state and the C–C reductive elimination from a d^{n-2} -metal intermediate.⁸ For a rhodium catalyst, these reactions can be ordered according to the tentative cycle shown in Scheme 1. Thus, the design of the optimal catalyst requires sequencing the splitting of the σ -bonds and the C–C bond formation, in the metal coordination sphere, for which an adequate difference between the activation energies of such elemental steps is crucial. The success of the cross-coupling demands a deep knowledge of the factors governing such reactions.

Halides are versatile functional groups; organic halides are classified as core building blocks in organic synthesis.⁹ In the

Scheme 1. Elemental Steps for the Rhodium-Promoted C–H Arylation

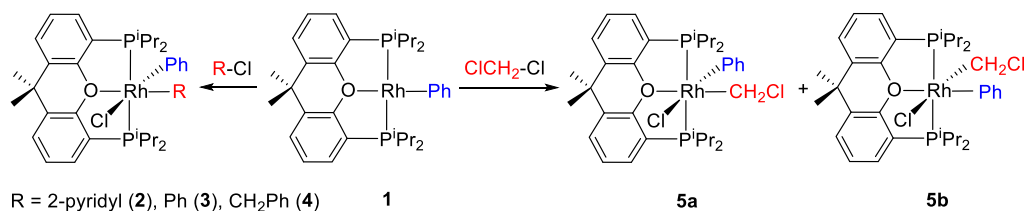


Received: November 17, 2021

Published: March 17, 2022



Scheme 2. Oxidative Addition Reactions



catalytic cycle shown in Scheme 1, a square-planar rhodium(I)-aryl complex **A** undergoes oxidative addition of a C–X (X = Cl, Br, and I) bond of an organic halide. The **A**-type complexes are hardly isolable and therefore their number is scarce,¹⁰ and as a consequence, the study of this first step of the cycle is a challenge, which as far as we know has not been addressed. Nevertheless, in agreement with the catalytic rhodium use in the C–H arylation, the oxidative addition of C–X bonds to other rhodium(I) complexes has attracted notable interest, in particular, the reactions involving C(sp²)–Cl^{10d,i,11} and C(sp³)–Cl¹² additions. Although the C–X bond strength decreases on going down to group 17, the organic chlorides are more interesting substrates than bromides and iodides by their lower cost and wider diversity. Once formed, the six-coordinate rhodium(III) intermediate **B**, bearing two single Rh–C bonds, the subsequent halide dissociation should allow an unsaturated five-coordinate species **C**, which would undergo C–C reductive elimination to generate the product of the catalysis. The latter is certainly the critical step in the cross-coupling process. However, in spite of its relevance, many basic questions about the factors that govern it remain largely unanswered. The importance of the five-coordinate intermediates is well-established for the C–C reductive elimination in platinum(IV) complexes, from both experimental¹³ and theoretical¹⁴ points of view. For a five-coordinate species, trigonal bipyramids or square pyramids are the usual polyhedrons defined by the donor atoms of the ligands around the metal center. The C–C reductive elimination is stereocontrolled; for the trigonal bipyramid arrangement, the coupling of two equatorial groups is favored with regard to the axial-equatorial coupling, while for the square pyramid disposition, the coupling of basal and axial ligands is favored with regard to the coupling of two basal groups. Thus, the electronic nature of the ligands along with their rigidity or flexibility, which ascertain the donor atom disposition around the metal center and constrain the interconversion between the polyhedrons, is a crucial factor for the C–C coupling, in particular, when pincer groups are used to stabilize the system.¹⁵ Because such five-coordinate species are the key for understanding the C–C coupling, their isolation and study should be an imperative target, but unfortunately, they display scarce stability and have been rarely isolated.^{11a,16} In the presence of an arene, the C–C reductive elimination should afford a rhodium(I)-arene derivative **D**, which would evolve to the hydride-rhodium(III)-aryl intermediate **E** by oxidative addition of one C(sp²)–H bond of the arene. Thus, the deprotonation of the metal center of **E** could regenerate the square-planar rhodium(I)-aryl complex **A**. The Brønsted–Lowry acid character of cationic transition metal-hydride compounds is well-known.¹⁷

Weller's group has proved that POP diphosphines are hemilabile ligands.¹⁸ In 2010, we prepared 9,9-dimethyl-4,5-bis(diisopropylphosphino)xanthene (xant(PⁱPr₂)₂), among

other ether diphosphines.¹⁹ This ligand displays more coordinating flexibility than the classical POP diphosphines. Thus, species with the ligand bonded in the modes κ²-P,P-*cis* and κ²-P,P-*trans*, which prove the hemilabile character of the oxygen atom, are also known in this case.²⁰ However, the pincer κ³-P,O,P-*mer* coordination is the most usual,^{10g–i,12g,21} although complexes bearing the diphosphine κ³-P,O,P-*fac*-coordinated have been additionally reported.^{20e,22} Accordingly, diphosphine xant(PⁱPr₂)₂ allows structural changes in its complexes, to adapt the metal coordination sphere to the needs of the reactions. As a result, a number of metal derivatives stabilized by this ligand have proven to be active catalysts for a range of interesting organic transformations,^{10h,20a,d,21b,f–h,23} including cross-coupling reactions that involve elemental steps of σ-bond activation in both substrates such as the borylation^{10g,24} and silylation²⁵ of arenes. As a part of the chemistry of the Rh-xant(PⁱPr₂)₂ moiety, we have previously reported that the square-planar rhodium(I)-hydride complex RhH{κ³-P,O,P-[xant(PⁱPr₂)₂]} activates C–H and C–Cl bonds of arenes to afford the corresponding rhodium(III) species RhH₂(aryl){κ³-P,O,P-[xant(PⁱPr₂)₂]} and RhH(aryl)Cl{κ³-P,O,P-[xant(PⁱPr₂)₂]}, which eliminate H₂ and HCl, respectively, to form a wide variety of square-planar derivatives Rh(aryl){κ³-P,O,P-[xant(PⁱPr₂)₂]}.^{10g,i} The coordinating flexibility of xant(PⁱPr₂)₂, the success of some of its metal derivatives as catalysts for cross-coupling reactions formed by elemental steps involving σ-bond activation-coupling, and the easy accessibility to **A**-type complexes prompted us to study two key steps of the cycle shown in Scheme 1, the oxidative addition of C(sp²)–Cl and C(sp³)–Cl bonds to **A** and the C–C reductive elimination from **C** in the presence of an arene, for four substrates: 2-chloropyridine, chlorobenzene, benzyl chloride, and dichloromethane.

This paper shows a comparative study about the oxidative addition of the previously mentioned substrates to the aryl complex RhPh{κ³-P,O,P-[xant(PⁱPr₂)₂]}, the transformation of the resulting six-coordinate derivatives into five-coordinate species, and the C–C reductive elimination from the unsaturated compounds, in the presence of fluorobenzene, also in a comparative manner.

RESULTS AND DISCUSSION

Oxidative Addition Reactions. The behavior of the square-planar rhodium(I) complex RhPh{κ³-P,O,P-[xant(PⁱPr₂)₂]} (**1**) toward 2-chloropyridine, chlorobenzene, benzyl chloride, and dichloromethane is summarized in Scheme 2.

The reactions were not influenced by light neither by the presence of 5 mol % of hydroquinone. According to such findings, radicals do not appear to play any role during the processes. Stirring of **1** in 2-chloropyridine, at 50 °C, for 48 h gives rise to one rhodium(III) stereoisomer of those possible for the formula Rh(Ph)(2-pyridyl)Cl{κ³-P,O,P-[xant(PⁱPr₂)₂]} (**2**). This species is generated as a result of the oxidative

addition of the C(sp²)-Cl bond of the solvent to the metal center of **1**. Complex **2** was isolated as a yellow solid in 56% and characterized by X-ray diffraction analysis. In accordance with the stereochemistry depicted in Scheme 2 for **2**, the structure (Figure 1) reveals that the isolated isomer bears a

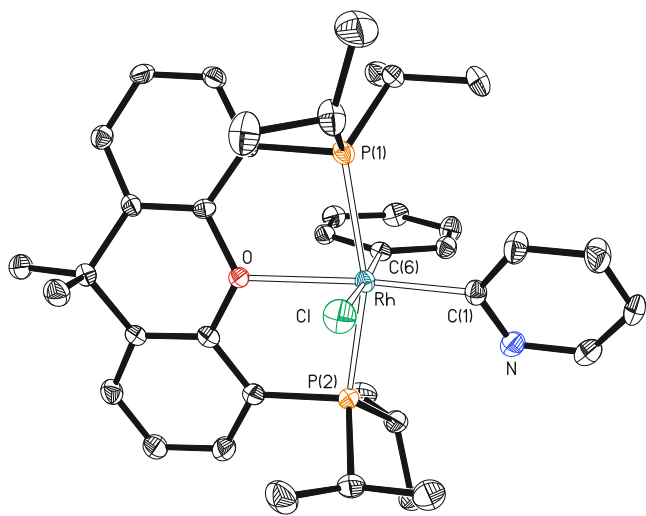


Figure 1. Molecular diagram of complex **2** (ellipsoids shown at 50% probability). All hydrogen atoms are omitted for clarity. Selected bond distances (Å) and angles (°): Rh–P(1) = 2.3541(7), Rh–P(2) = 2.3071(7), Rh–Cl = 2.4520(7), Rh–C(1) = 1.995(2), Rh–C(6) = 2.055(2), Rh–O = 2.2874(16); P(1)–Rh–P(2) = 161.39(2), Cl–Rh–C(1) = 88.01(7), Cl–Rh–C(6) = 177.12(7), O–Rh–C(1) = 173.56(8), and C(1)–Rh–C(6) = 93.67(10).

pyridyl-*trans*-oxygen disposition (O–Rh–C(1) = 173.56(9)°). Thus, the polyhedron around the rhodium atom can be idealized as the expected octahedron with the ether-diphosphine *mer*-coordinated and the chloride ligand disposed *trans* to the phenyl group. The NMR spectra (Figures S31–S33) in benzene-*d*₆ are consistent with this ligand disposition. In agreement with the equivalence of the PⁱPr₂ groups of the pincer, the ³¹P{¹H} spectrum shows a doublet (¹J_{P–Rh} = 119 Hz) at 27.7 ppm. In the ¹³C{¹H} spectrum, the resonances corresponding to the metalated carbon atoms are observed at 143.7 (Ph) and 173.9 (pyridyl) ppm as doublets of triplets with C–Rh and C–P coupling constants of 34 and 40 Hz and 10 and 6 Hz, respectively.

The reaction of **1** with chlorobenzene was also performed in the neat organic halide as a solvent, in this case at 90 °C. Under these conditions, the oxidative addition product RhPh₂Cl{κ³-P,O,P-[xant(PⁱPr₂)₂]} (**3**) was obtained as a yellowish white solid in 76% yield, after 48 h. Its structure (Figure 2) resembles that of **2** with one of the phenyl ligands in the position of the pyridyl group, disposed *trans* to the oxygen atom of the diphosphine (O–Rh–C(1) = 177.50(7)°). In agreement with the presence of two inequivalent phenyl ligands in the complex, the ¹³C{¹H} NMR spectrum (Figure S36) in benzene-*d*₆ displays two doublets (¹J_{C–Rh} = 39 and 33 Hz) of triplets (²J_{C–P} = 9 and 8 Hz) at 146.4 (*trans* to Cl) and 152.7 (*trans* to O) ppm. In accordance with **2**, the ³¹P{¹H} NMR spectrum (Figure S35) shows a doublet (¹J_{P–Rh} = 114 Hz) at 26.5 ppm, for the equivalent PⁱPr₂ groups of the pincer.

The C(sp³)-Cl oxidative additions to **1** seem to have activation barriers lower than the additions of a C(sp²)-Cl bond. In contrast to 2-chloropyridine and chlorobenzene,

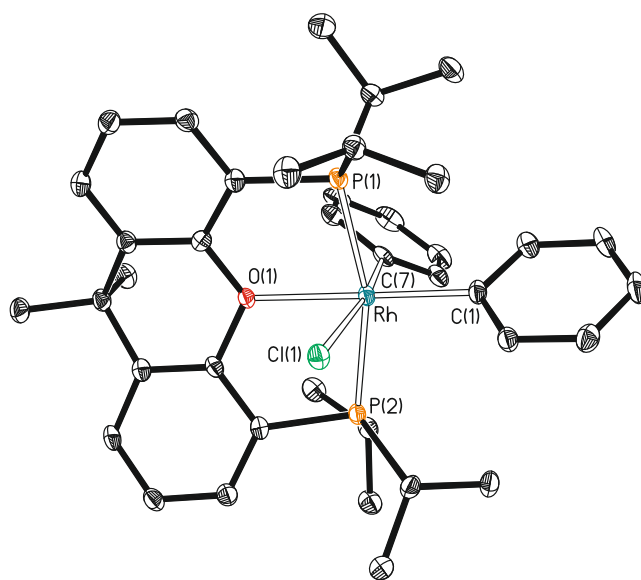


Figure 2. Molecular diagram of complex **3** (ellipsoids shown at 50% probability). All hydrogen atoms are omitted for clarity. Selected bond distances (Å) and angles (°): Rh–P(1) = 2.3164(6), Rh–P(2) = 2.3472(6), Rh–Cl(1) = 2.5058(6), Rh–C(1) = 2.0348(18), Rh–C(7) = 2.0382(19), Rh–O(1) = 2.2448(13); P(1)–Rh–P(2) = 162.736(18), Cl(1)–Rh–C(1) = 97.25(6), Cl(1)–Rh–C(7) = 169.20(5), O(1)–Rh–C(1) = 177.50(6), and C(1)–Rh–C(7) = 93.17(7).

benzyl chloride instantaneously reacts with **1**, at room temperature, even using stoichiometric amounts of the reagents. The oxidative addition product, the benzyl-aryl complex RhPh(CH₂Ph)Cl{κ³-P,O,P-[xant(PⁱPr₂)₂]} (**4**), was isolated as a white solid in 80% yield and characterized by X-ray diffraction analysis. The structure (Figure 3) is consistent with that of **2**, showing that the generated benzyl ligand is disposed *trans* to the oxygen atom of the pincer (O–Rh–C(1) = 169.64(7)°). The ¹H and ¹³C{¹H} NMR spectra (Figures S37 and S39) in benzene-*d*₆ are consistent with the presence of the benzyl ligand in the complex. Thus, the ¹H spectrum shows a doublet (²J_{H–Rh} = 3.2 Hz) of triplets (³J_{H–P} = 3.6 Hz) at 5.02 ppm, which fits with other doublet (¹J_{C–Rh} = 29 Hz) of triplets (²J_{C–P} = 5 Hz) at 16.8 ppm in the ¹³C{¹H} spectrum, both due to the CH₂ group. In accordance with **2** and **3**, the ¹³C{¹H} spectrum also contains a doublet (¹J_{C–Rh} = 33 Hz) of triplets (²J_{C–P} = 11 Hz) at 141.9 ppm, corresponding to the metalated carbon atom of the phenyl ligand, whereas the ³¹P{¹H} spectrum (Figure S38) displays a doublet (¹J_{P–Rh} = 118 Hz) at 22.4 ppm for the equivalent PⁱPr₂ groups of the diphosphine.

Complexes **2–4** are the result of a *cis*-addition of the C–Cl bond of the organic chlorides to **1**. Keeping the pincer skeleton, this addition could in principle take place in a direct manner or by steps (Scheme 3). The direct form involves a concerted addition along the O–Rh–Ph axis, with the chlorine substituent of the substrate above the oxygen atom of the diphosphine (a). The addition by steps should be initiated by an S_N2-type rupture and requires a thermodynamic control of the stereochemistry (b); the five-coordinate intermediate resulting from the C–Cl rupture (F; R *trans* to the coordination vacancy) would undergo an isomerization process of a low activation barrier, which could involve a phenyl shift of 90° in the perpendicular plane to the P–Rh–P direction to afford a new five-coordinate square pyramidal

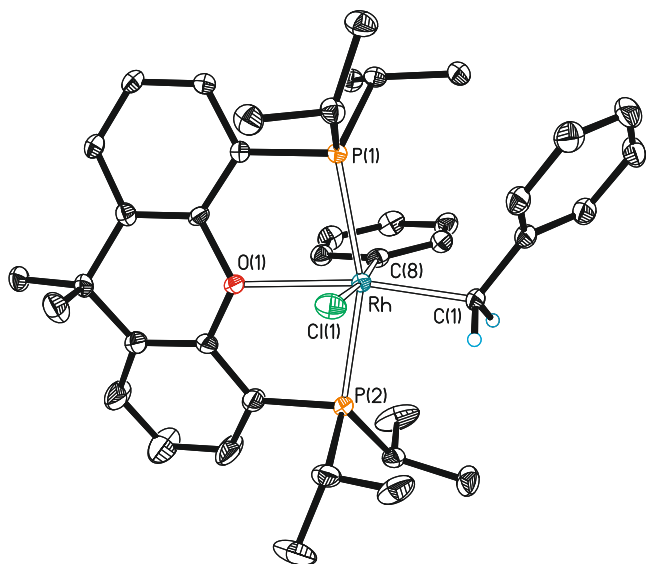


Figure 3. Molecular diagram of complex **4** (ellipsoids shown at 50% probability). All hydrogen atoms (except those of the CH₂ moiety) are omitted for clarity. Selected bond distances (Å) and angles (°): Rh–P(1) = 2.3578(6), Rh–P(2) = 2.3206(6), Rh–Cl(1) = 2.4682(6), Rh–C(1) = 2.091(2), Rh–C(8) = 2.053(2), Rh–O(1) = 2.3217(15); P(1)–Rh–P(2) = 160.93(2), Cl(1)–Rh–C(1) = 90.71(7), Cl(1)–Rh–C(8) = 174.90(6), O(1)–Rh–C(1) = 169.64(7), and C(1)–Rh–C(8) = 93.00(9).

intermediate **G**, with the diphosphine oxygen atom trans to the coordination vacancy, followed by an R shift of 90° to locate the added organic fragment trans to the oxygen atom and cis to the coordination vacancy. In this way, the entry of the chloride in the coordination vacancy of **H** could give the obtained compounds.

The oxidative addition of one of the C(sp³)–Cl bonds of dichloromethane to **1** shows significant differences with regard to the reaction with benzyl chloride. It must be performed in the halide as a solvent or using a great excess and leads to two different isomers of formula RhPh(CH₂Cl)Cl{κ³-P,O,P-[xant-(PⁱPr₂)₂]} (**5a** and **5b**) in a 1.1:1 molar ratio. For one of them, **5b**, crystals suitable for X-ray diffraction analysis were

obtained. Its structure (Figure 4) revealed a mutually trans disposition for the added fragments (Cl(1)–Rh(1)–C(7) =

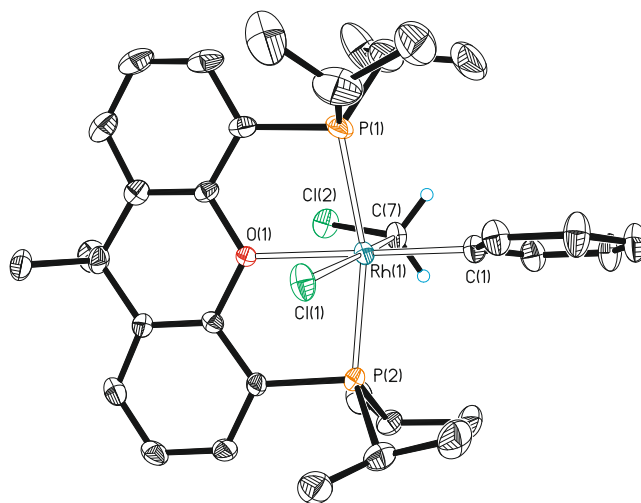
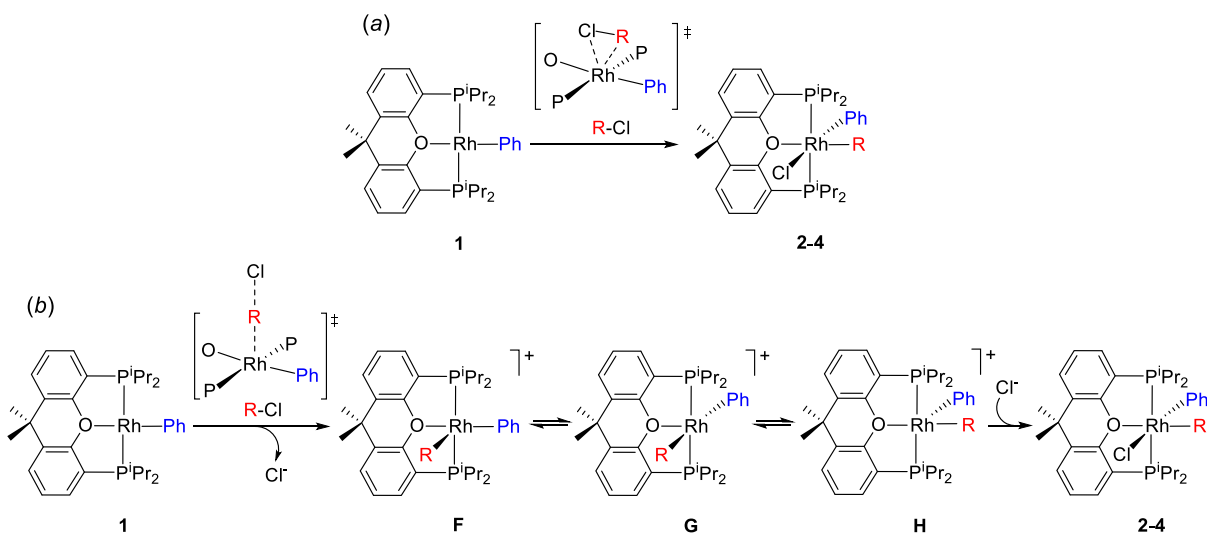


Figure 4. Molecular diagram of complex **5b** (ellipsoids shown at 50% probability). All hydrogen atoms (except those of the CH₂ moiety) are omitted for clarity. Selected bond distances (Å) and angles (°): Rh(1)–P(1) = 2.3191(14), 2.3312(13), Rh(1)–P(2) = 2.3361(13), 2.3412(12), Rh(1)–Cl(1) = 2.4966(13), 2.4893(14), Rh(1)–C(1) = 2.028(5), 2.029(5), Rh(1)–C(7) = 2.042(5), 2.054(5), Rh(1)–O(1) = 2.222(3), 2.241(3); P(1)–Rh(1)–P(2) = 164.74(5), 163.76(5), Cl(1)–Rh(1)–C(1) = 98.25(15), 97.42(16), Cl(1)–Rh(1)–C(7) = 173.04(15), 174.19(16), O(1)–Rh(1)–C(1) = 176.50(17), 176.45(17), C(1)–Rh(1)–C(7) = 88.5(2), 88.4(2).

173.04(15) and 174.19(16)°.²⁶ The formation of two isomers is strongly supported by the NMR spectra (Figures S40–S42), in dichloromethane-*d*₂, at room temperature. The ¹H spectrum shows two CH₂Cl resonances at 5.76 and 4.79 ppm, which are observed as doublets of triplets with H–Rh and H–P coupling constants of about 3 and 7 Hz, respectively. The resonance at the lower field was assigned to isomer **5a** (CH₂Cl trans to O) on the base of the stronger *trans*-effect of ether regarding chloride.²⁷ The ¹³C{¹H} spectrum contains two sets of two doublets of triplets; one of them close to 141 ppm (¹J_{C–Rh} ≈ 35 Hz, ²J_{C–P} = 10 Hz) due to the metalated carbon atom of the

Scheme 3. Plausible Mechanisms for the Formation of Complexes 2–4



phenyl ligand and the other around 40 ppm ($^1J_{C-Rh} \approx 35$ Hz, $^2J_{C-P} \approx 7$ Hz) corresponding to the CH_2Cl group. Doublets at 27.5 ($^1J_{P-Rh} = 114$ Hz) and 27.3 ($^1J_{P-Rh} = 110$ Hz) ppm in the $^{31}P\{^1H\}$ spectrum are also features of these species. Once the mixture is formed, its composition does not change with the temperature, indicating that the isomerization between **5a** and **5b** is not kinetically accessible.

The previous observations in a qualitative manner point out that the activation barrier for the oxidative addition increases in the sequence benzyl chloride < dichloromethane < 2-chloropyridine < chlorobenzene and that the cis addition of the C–Cl bond is favored with regard to the trans one; thus, only in the dichloromethane case, both types of additions are observed. In addition, it should be noted that the chloride-*trans*-oxygen disposition is elusive. The presence of two π -donor groups on the same metal orbital most probably produces a decrease in the stability of such isomers with regard to those observed, which bear a chloride-*trans*-phenyl disposition. In order to quantitatively confirm the activation barrier sequence and to gain information of the intimate details of the additions, we studied the kinetics of the reactions of 2-chloropyridine, chlorobenzene, and dichloromethane, those occurring at rates that allow the study, by $^{31}P\{^1H\}$ NMR spectroscopy.

The oxidative additions of 2-chloropyridine and chlorobenzene to **1** in the neat organic halide as a solvent are pseudo-first-order processes, which fit to the expression shown in eq 1, where $[1]_0$ is the initial concentration of **1** and $[1]$ is the concentration at the time t . The values of the observed k_1 in the temperature range studied are gathered in Table 1. The

Table 1. Rate Constants (k_1 , s^{-1}) for the Formation of Complexes **2** and **3**

complex 2		complex 3	
T (K)	k_1 (s^{-1})	T (K)	k_1 (s^{-1})
323	$(9.6 \pm 0.6) \times 10^{-5}$	363	$(1.8 \pm 0.2) \times 10^{-5}$
328	$(1.5 \pm 0.1) \times 10^{-4}$	373	$(3.6 \pm 0.2) \times 10^{-5}$
333	$(1.9 \pm 0.2) \times 10^{-4}$	383	$(4.6 \pm 0.4) \times 10^{-5}$
338	$(2.3 \pm 0.2) \times 10^{-4}$	393	$(8.7 \pm 0.6) \times 10^{-5}$
343	$(3.1 \pm 0.2) \times 10^{-4}$	398	$(1.0 \pm 0.1) \times 10^{-4}$

activation parameters obtained from the respective Eyring analysis (Figures S6 and S12) are $\Delta H^\ddagger = 11.6 \pm 2.2$ kcal mol^{-1} , $\Delta S^\ddagger = -41.1 \pm 6.5$ cal $K^{-1} mol^{-1}$, and $\Delta G_{298}^\ddagger = 23.8 \pm 4.1$ kcal mol^{-1} for 2-chloropyridine and $\Delta H^\ddagger = 13.3 \pm 1.6$ kcal mol^{-1} , $\Delta S^\ddagger = -44.0 \pm 4.2$ cal $K^{-1} mol^{-1}$, and $\Delta G_{298}^\ddagger = 26.4 \pm 2.9$ kcal mol^{-1} for chlorobenzene. The marked negative values of the activation entropy are consistent with a concerted addition along the O–Rh–Ph axis with the aromatic ring of the organic halide on the phenyl group (a in Scheme 3). Thus, π – π interactions between the aromatic rings could contribute to increase the order in the transition state.

$$\ln \frac{[1]}{[1]_0} = -k_1 t \quad (1)$$

Figure 5 shows the $^{31}P\{^1H\}$ NMR spectra of the addition of dichloromethane to **1**, as a function of time, under pseudo-first-order conditions (20 equiv CH_2Cl_2), at 288 K. The dependence of the concentrations of **1**, **5a**, and **5b** with time (Figure 6) fits to the expressions shown in eqs 2–4, respectively, which rationalize two parallel reactions²⁸ in

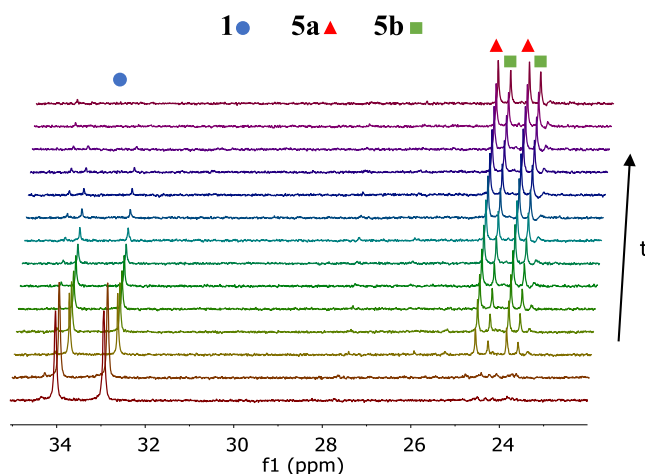


Figure 5. Stacked $^{31}P\{^1H\}$ NMR spectra (161.98 MHz, toluene- d_6 , 288 K) showing the reaction of **1** with dichloromethane as a function of time.

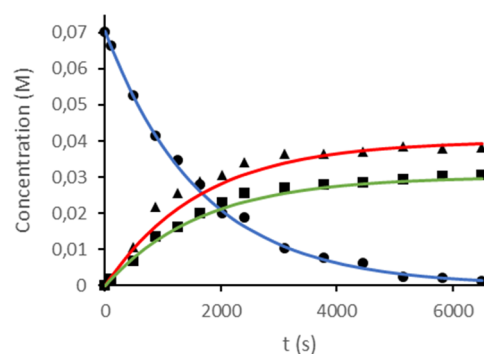


Figure 6. Composition of the mixture as a function of time for the reaction of **1** with dichloromethane at 288 K (**1**, black ●; **5a** black ▲; and **5b** black ■). Fits to eqs 2–4 are given in color.

agreement with two different oxidative additions. The values of k_{5a} and k_{5b} in the temperature range studied are collected in Table 2. The activation parameters calculated from the

Table 2. Rate Constants k_{5a} and k_{5b} (s^{-1}) for the Reaction of **1** with Dichloromethane

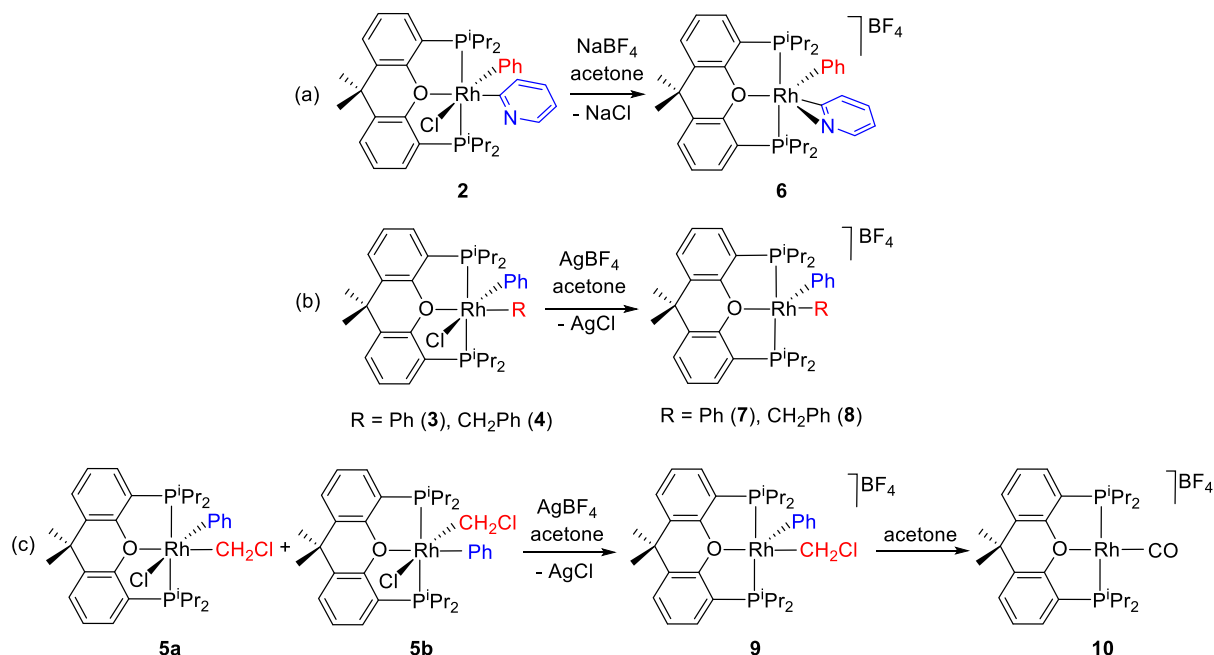
T (K)	k_{5a} (s^{-1})	k_{5b} (s^{-1})
268	$(6.2 \pm 0.3) \times 10^{-5}$	$(3.6 \pm 0.3) \times 10^{-5}$
273	$(8.3 \pm 0.5) \times 10^{-5}$	$(6.4 \pm 0.6) \times 10^{-5}$
278	$(1.2 \pm 0.6) \times 10^{-4}$	$(8.0 \pm 0.5) \times 10^{-5}$
288	$(3.5 \pm 0.2) \times 10^{-4}$	$(2.6 \pm 0.3) \times 10^{-4}$
298	$(7.6 \pm 0.9) \times 10^{-4}$	$(6.2 \pm 0.9) \times 10^{-4}$

corresponding Eyring analysis (Figures S18 and S19) are $\Delta H^\ddagger = 13.2 \pm 1.2$ kcal mol^{-1} , $\Delta S^\ddagger = -28.4 \pm 4.1$ cal $K^{-1} mol^{-1}$, and $\Delta G_{298}^\ddagger = 21.7 \pm 2.4$ kcal mol^{-1} for **5a** and $\Delta H^\ddagger = 14.5 \pm 1.2$ kcal mol^{-1} , $\Delta S^\ddagger = -24.5 \pm 4.4$ cal $K^{-1} mol^{-1}$, and $\Delta G_{298}^\ddagger = 21.8 \pm 2.6$ kcal mol^{-1} for **5b**.

$$[1] = [1]_0 e^{-(k_{5a} + k_{5b})t} \quad (2)$$

$$[5a] = \frac{k_{5a}}{k_{5a} + k_{5b}} [1]_0 (1 - e^{-(k_{5a} + k_{5b})t}) \quad (3)$$

Scheme 4. Abstraction of the Chloride Ligand



$$[\mathbf{5b}] = \frac{k_{5b}}{k_{5a} + k_{5b}} [\mathbf{1}]_0 (1 - e^{-(k_{5a} + k_{5b})t}) \quad (4)$$

The results of the kinetic analysis prove the existence of two independent oxidative additions of dichloromethane to **1** and confirm the activation barrier sequence qualitatively deduced. In this context, it should be mentioned that the activation energy sequence provided by this study agrees nicely with the sequence built with the C–Cl bond dissociation energies (kcal mol⁻¹) previously reported for the employed organic halides:²⁹ benzyl chloride (71.7 ± 1.1) < dichloromethane (80.8 ± 0.8) < 2-chloropyridine (90.5 ± 3.5) < chlorobenzene (95.5 ± 3.5). This suggests that the rate of the oxidative addition of organic chlorides to **1** significantly depends upon the strength of the C–Cl bond.

Five-Coordinate Rhodium(III) Complexes. Complexes **2**–**5** are stable in fluorobenzene, at 80 °C, for at least 1 week. Reductive C–C elimination was not observed in any case, which can be in principle attributed to the six-coordinate character of these compounds and a low tendency to dissociate the chloride ligand.^{11a,16} In view of it, we decided its abstraction with NaBF₄ in the case of **2** and AgBF₄ for **3**–**5**, in acetone, at room temperature. In contrast to Ag⁺, the Na⁺ ion prevents pyridine–cation interactions that could complicate the abstraction. Three different behaviors are observed depending on the organic halide added to **1** (Scheme 4): (a) 2-chloropyridine (**2**), (b) chlorobenzene (**3**) and benzyl chloride (**4**), and (c) dichloromethane (**5**).

Treatment of the acetone solutions of **2** with 1.0 equiv of NaBF₄ leads to the salt [RhPh{η²-C,N-(NC₅H₄)}{κ³-P,O,P-[xant(PⁱPr₂)₂]}]BF₄ (**6**), where the metal center of the cation saturates its electron deficiency by means of the coordination of the nitrogen atom of the pyridyl group. The salt was isolated as a white solid in 90% yield and characterized by X-ray diffraction analysis. The structure (Figure 7) proves the η²-C,N-coordination of the pyridyl group. Such a coordination mode is relatively usual for early metals³⁰ but is very rarely observed in complexes of platinum group metals.³¹ It generates

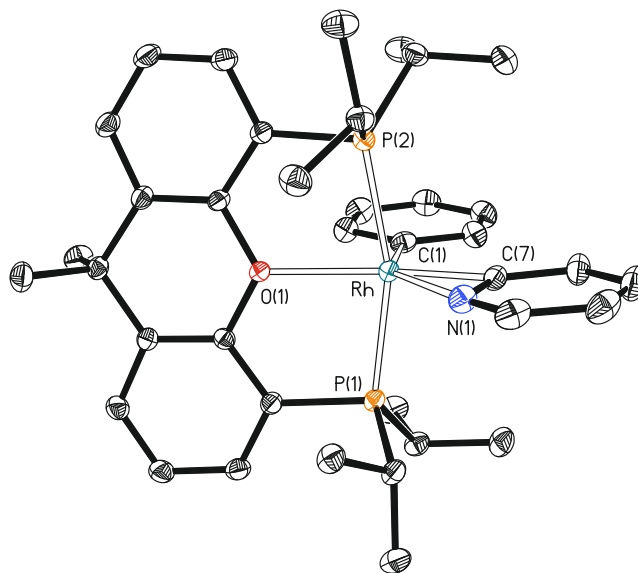


Figure 7. Molecular diagram of the cation of complex **6** (ellipsoids shown at 50% probability). All hydrogen atoms are omitted for clarity. Selected bond distances (Å) and angles (°): Rh–P(1) = 2.3177(11), Rh–P(2) = 2.3071(10), Rh–C(1) = 2.0133(17), Rh–C(7) = 1.9495(17), Rh–N(1) = 2.3483(16), Rh–O(1) = 2.2310(14); P(1)–Rh–P(2) = 163.201(16), O(1)–Rh–C(1) = 91.94(6), O(1)–Rh–C(7) = 160.07(6), C(1)–Rh–C(7) = 107.93(7), N(1)–Rh–C(7) = 34.49(6), O(1)–Rh–M = 141.21(6), C(1)–Rh–M = 126.82(6), where M is the midpoint of the C(7)–N(1) bond.

a 3e-donor ligand. Thus, the coordination polyhedron around the metal center can be described as a trigonal bipyramid with inequivalent angles of 91.94(6) (O(1)–Rh–C(1)), 126.82(6) (C(1)–Rh–M), and 141.21(6) (O(1)–Rh–M) in the Y-shaped equatorial plane, which is formed by the oxygen atom of the diposphine (O(1)), the metalated carbon atom of the phenyl ligand (C(1)), and the midpoint of the pyridyl C(7)–N(1) bond (M). The NMR spectra of the cation (Figures S43–S45) in dichloromethane-*d*₂ are consistent with the structure shown

in Figure 7. The $^31\text{P}\{^1\text{H}\}$ spectrum shows a doublet ($^1J_{\text{P-Rh}} = 113$ Hz) at 37.2 ppm, in agreement with the equivalence of the P^iPr_2 groups. In the $^{13}\text{C}\{^1\text{H}\}$ spectrum, the resonances assigned to the metalated carbon atoms are observed at 158.0 (pyridyl) and 135.4 (Ph) ppm, as doublets of triplets with C–Rh and C–P coupling constants of 34 and 44 Hz and 8 and 9 Hz, respectively.

The abstraction of the chloride ligand of **3** and **4** with AgBF_4 affords salts $[\text{RhPhR}\{\kappa^3\text{-P,O,P-[xant(P}^i\text{Pr}_2)_2]\}] \text{BF}_4$ (R = Ph (**7**), CH_2Ph (**8**)), which were isolated as yellow solids in almost quantitative yields. The five-coordinate unsaturated character of the cations, achieved in spite of the coordinating ability of the anion of the salts³² and the reaction solvent is noticeable. Particularly, remarkable is that of cation of **8**, which prefers to coordinate the benzyl group as $\kappa^1\text{-C}$ instead of the usual benzoallyl form for unsaturated centers.³³ The unsaturated nature of the cation of **8** was confirmed by X-ray diffraction analysis. Figure 8 gives a view of the structure,

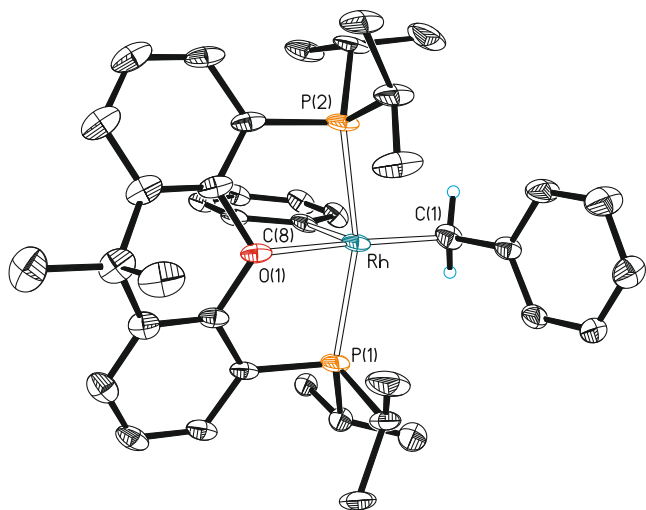


Figure 8. Molecular diagram of the cation of complex **8** (ellipsoids shown at 30% probability). All hydrogen atoms (except those of the CH_2 moiety) are omitted for clarity. Selected bond distances (Å) and angles ($^\circ$): Rh–P(1) = 2.3283(10), Rh–P(2) = 2.3351(10), Rh–C(1) = 2.058(5), Rh–C(8) = 2.021(4), Rh–O(1) = 2.307(3); P(1)–Rh–P(2) = 159.71(5), O(1)–Rh–C(1) = 170.28(13), O(1)–Rh–C(8) = 97.10(14), C(1)–Rh–C(8) = 92.62(17).

which proves the $\kappa^1\text{-C}$ coordination of the benzyl group. The polyhedron around the rhodium atom can be described as a distorted square pyramid with the phenyl ligand, displaying the strongest trans influence,²⁷ at the apex. The benzyl group lies at the base disposed trans to the oxygen atom of the diphosphine ($\text{C}(1)\text{-Rh-O}(1) = 170.28(13)^\circ$). In solution, the cations only have a rigid structure at low temperatures. At room temperature, the C-donor ligands undergo a position exchange involving sequential shifts of about 90° in the perpendicular plane to the P–Rh–P direction (see b in Scheme 3). Thus, at room temperature, the $^{13}\text{C}\{^1\text{H}\}$ NMR spectrum of **7** in dichloromethane- d_2 shows a doublet ($^1J_{\text{C-Rh}} = 41$ Hz) of triplets ($^2J_{\text{C-P}} = 8$ Hz) at 141.7 ppm, corresponding to the metalated carbon atoms of the phenyl groups (Figure S48). This signal splits into two resonances at 146 and 138 ppm in the spectrum at 183 K (Figure S49). In the $^{13}\text{C}\{^1\text{H}\}$ spectrum of **8**, at 233 K, the resonances due to

metalated carbon atoms are observed at 131.1 (Ph) and 22.6 (CH_2Ph) ppm (Figure S52).

The addition of 1.0 equiv of AgBF_4 to acetone solutions of the isomeric mixture of **5a–5b** produces the abstraction of the chloride ligand to initially afford the salt $[\text{RhPh}(\text{CH}_2\text{Cl})\{\kappa^3\text{-P,O,P-[xant(P}^i\text{Pr}_2)_2]\}] \text{BF}_4$ (**9**), a chloromethyl counterpart of **7** and **8**. In a consistent manner with them, its $^{13}\text{C}\{^1\text{H}\}$ NMR spectrum (Figure S55) at 253 K displays two doublets of triplets at 135.1 ($^1J_{\text{C-Rh}} = 44$ Hz, $^2J_{\text{C-P}} = 9$ Hz) and 45.5 ($^1J_{\text{C-Rh}} = 34$ Hz, $^2J_{\text{C-P}} = 7$ Hz) ppm, corresponding to the metalated carbon atoms of the phenyl and chloromethyl ligands, respectively. However, in contrast to **7** and **8**, the cation of **9** is unstable in acetone, transforming into the carbonyl derivative $[\text{Rh}(\text{CO})\{\kappa^3\text{-P,O,P-[xant(P}^i\text{Pr}_2)_2]\}] \text{BF}_4$ (**10**), as a consequence of the rhodium-promoted solvent decarbonylation. At 70°C , the metal carbonylation is completed after 24 h. Salt **10** was isolated as a yellow solid in 87% yield. The presence of the carbonyl group at the cation is strongly supported by the IR, which contains a characteristic strong $\nu(\text{CO})$ band at 1978 cm^{-1} , and the $^{13}\text{C}\{^1\text{H}\}$ spectrum (Figure S58) shows the expected CO resonance at 191.5 ppm as a doublet of triplets with C–Rh and C–P coupling constants of 86 and 14 Hz. The metal-mediated decarbonylation of aldehydes is a well-known and trivial reaction,³⁴ but the carbonyl abstraction from ketones is only rarely observed with very particular systems.³⁵

C–C Reductive Elimination Reactions. The electron saturation of the metal center of **6** prevents the reductive elimination of 2-phenylpyridine. Complex **6** is stable in fluorobenzene, at 80°C , for at least 2 weeks. In contrast to the latter, the unsaturated compounds **7** and **8** eliminate biphenyl and benzylbenzene, respectively, under the same conditions. The resulting solvated fragment $[\text{Rh}(\eta^2\text{-C}_6\text{H}_5\text{F})\{\kappa^3\text{-P,O,P-[xant(P}^i\text{Pr}_2)_2]\}] \text{BF}_4$ (**1**) rapidly activates a C–H bond of the coordinated solvent³⁶ to give a 7:3 mixture of the *ortho*- and *meta*-fluorophenyl isomers $\text{RhH}(o\text{-C}_6\text{H}_4\text{F})(\kappa^1\text{-FBF}_3)\{\kappa^3\text{-P,O,P-[xant(P}^i\text{Pr}_2)_2]\}$ (**11a**) and $\text{RhH}(m\text{-C}_6\text{H}_4\text{F})(\kappa^1\text{-FBF}_3)\{\kappa^3\text{-P,O,P-[xant(P}^i\text{Pr}_2)_2]\}$ (**11b**). The transformation of **7** into the mixture of **11a** and **11b** is quantitative after 5 days, whereas only 2 days are necessary to convert **8** into the isomeric mixture. On the other hand, the same mixture is also rapidly formed when the chloride ligand of the square-planar rhodium(I) complex $\text{RhCl}\{\kappa^3\text{-P,O,P-[xant(P}^i\text{Pr}_2)_2]\}$ (**12**) is abstracted with AgBF_4 , in fluorobenzene, at room temperature (Scheme 5).

The coordination of the $[\text{BF}_4]^-$ anion to the metal center of **11a** and **11b** in the solid state was revealed by the FT-IR–ATR of the mixture, which displays the characteristic absorptions for a BF_4 -group with C_s symmetry³² at 1095, 953, and 745 cm^{-1} and the X-ray structure of **11a**, which proves the coordination index of six for its metal center (Figure 9). Thus, the polyhedron around the rhodium atom can be idealized as an octahedron with the diphosphine disposed in *mer*-fashion and a perpendicular plane to the P–Rh–P direction containing the hydride ligand disposed trans to the monodentate $[\text{BF}_4]^-$ anion and the fluorophenyl group situated trans to the oxygen atom of the pincer. In acetone solution, both isomers dissociate the $[\text{BF}_4]^-$ anion. This is strongly supported by the $^{19}\text{F}\{^1\text{H}\}$ NMR spectrum (Figure S62), which contains only one $[\text{BF}_4]^-$ resonance at -151.4 ppm, whereas the ^1H and $^{31}\text{P}\{^1\text{H}\}$ NMR spectra (Figures S59 and S60) do not display spin coupling with ^{19}F . Thus, even at 193 K, the first of them shows the hydride resonances as

Scheme 5. C–C Reductive Elimination Reactions

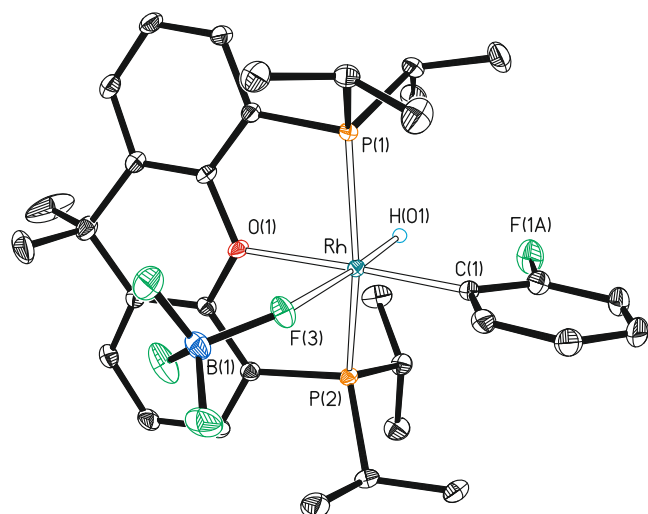
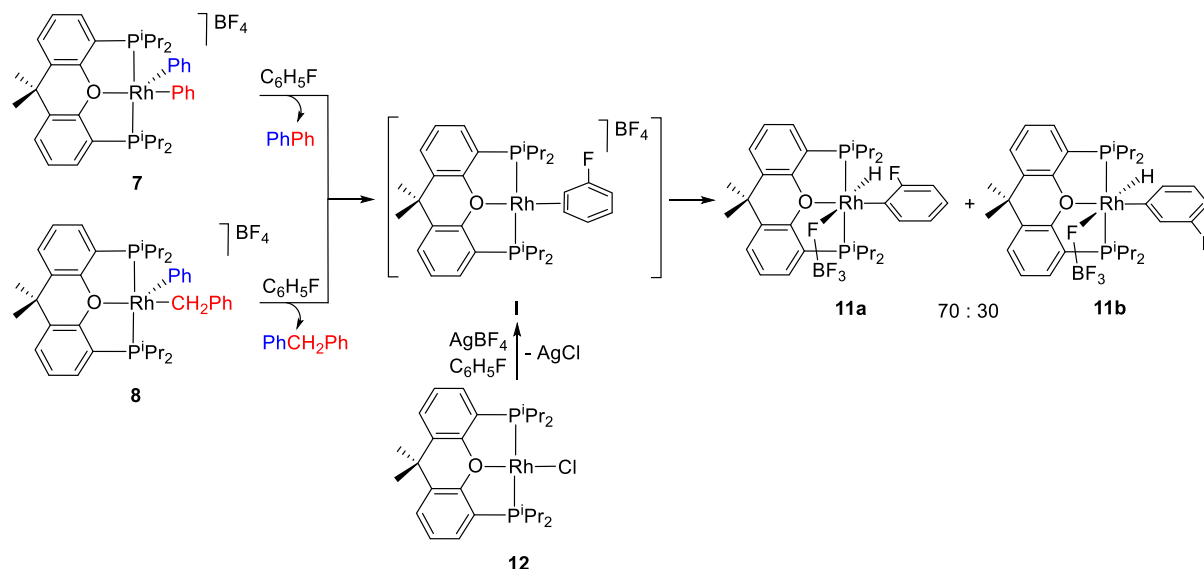


Figure 9. Molecular diagram of complex **11a** (ellipsoids shown at 50% probability). All hydrogen atoms (except the hydride) are omitted for clarity. Selected bond distances (Å) and angles (°): Rh–P(1) = 2.2964(4), Rh–P(2) = 2.2912(4), Rh–C(1) = 2.0009(13), Rh–O(1) = 2.2023(9), Rh–F(3) = 2.3551(9); P(1)–Rh–P(2) = 156.501(13), O(1)–Rh–C(1) = 177.90(5), H(01)–Rh–F(3) = 175.4(7), H(01)–Rh–C(1) = 84.6(6), C(1)–Rh–F(3) = 95.44(5).

doublets of triplets at -18.95 ($^1J_{\text{H-Rh}} = 30.6$ Hz, $^2J_{\text{H-P}} = 12.9$ Hz) ppm for **11a** and at -19.92 ($^1J_{\text{H-Rh}} = 35.5$ Hz, $^2J_{\text{H-P}} = 13.4$ Hz) ppm for **11b**. The second one, for its part, displays a single doublet for each isomer, at 43.6 ($^1J_{\text{P-Rh}} = 111$ Hz) ppm for **11a** and at 40.9 ($^1J_{\text{P-Rh}} = 115$ Hz) ppm for **11b**.

The extremely rapid formation of the isomeric mixture of **11a** and **11b**, by abstraction of the chloride ligand of **12** in fluorobenzene, indicates that the C–H bond activation of the coordinated fluorobenzene of **I** is much faster than C–C reductive elimination from the five-coordinate cations. This is consistent with the nonobservation of such an intermediate during the transformations of **7** and **8** into the isomeric mixture and points out that the C–C reductive elimination is the rate-determining step of the processes and therefore the step from which the activation parameters depend. Such

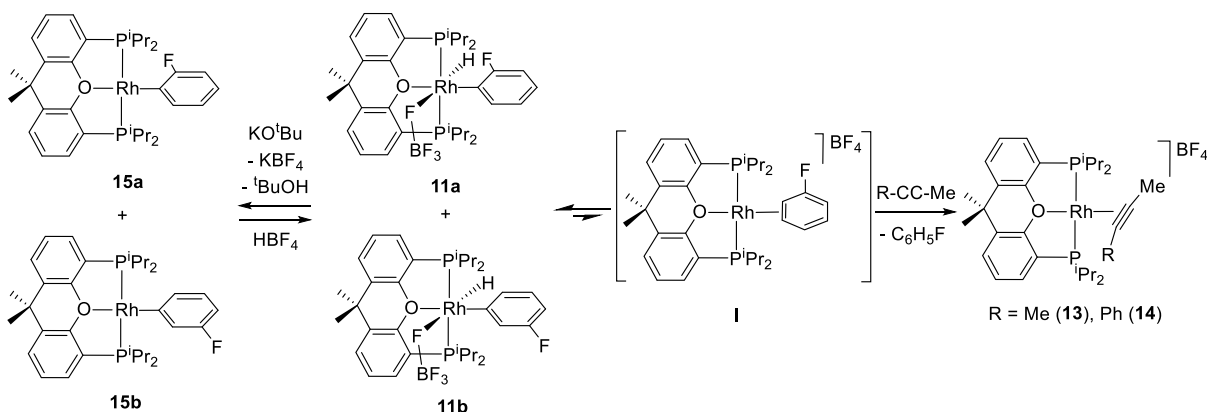
transformations were followed by $^{31}\text{P}\{^1\text{H}\}$ NMR spectroscopy. Decreases in **7** and **8** are first-order reactions, which can be described according to eq 5, where $[\text{M}]_0$ is the initial concentrations of the five-coordinate cations, whereas $[\text{M}]$ represents the concentrations at the time t . The values of k_{R} in the temperature range studied are collected in Table 3. The

Table 3. Rate Constants (k_{R} , s^{-1}) for the C–C Reductive Elimination Processes from Complexes **7** and **8**

complex 7		complex 8	
T (K)	k_{R} (s^{-1})	T (K)	k_{R} (s^{-1})
343	$(3.6 \pm 0.6) \times 10^{-6}$	338	$(1.1 \pm 0.3) \times 10^{-5}$
348	$(6.1 \pm 0.6) \times 10^{-6}$	353	$(1.8 \pm 0.8) \times 10^{-5}$
353	$(1.1 \pm 0.1) \times 10^{-5}$	358	$(1.9 \pm 0.4) \times 10^{-5}$
358	$(1.9 \pm 0.4) \times 10^{-5}$	363	$(2.3 \pm 0.7) \times 10^{-5}$
363	$(2.6 \pm 0.4) \times 10^{-5}$		

activation parameters for the respective C–C reductive eliminations, obtained from the corresponding Eyring analysis (Figures S25 and S30), are $\Delta H^\ddagger = 24.2 \pm 3.4$ kcal mol $^{-1}$, $\Delta S^\ddagger = -13.0 \pm 9.9$ cal K $^{-1}$ mol $^{-1}$, and $\Delta G_{298}^\ddagger = 28.1 \pm 6.4$ kcal mol $^{-1}$ for the reductive elimination of biphenyl and $\Delta H^\ddagger = 6.2 \pm 1.5$ kcal mol $^{-1}$, $\Delta S^\ddagger = -31.4 \pm 4.4$ cal K $^{-1}$ mol $^{-1}$, and $\Delta G_{298}^\ddagger = 15.6 \pm 2.9$ kcal mol $^{-1}$ for the reductive elimination of benzylbenzene. The lower activation enthalpy for the C(sp 3)–C(sp 2) reductive elimination respecting the C(sp 2)–C(sp 2) coupling is consistent with the smaller dissociation energy of the C(sp 3)–C(sp 2) bond of benzylbenzene with regard to the dissociation energy of the C(sp 2)–C(sp 2) single bond of biphenyl (91.7 ± 2.0 vs 114.4 ± 1.5 kcal mol $^{-1}$).²⁹ The marked negative values of the activation entropies agree well with the concerted character of the reductive eliminations, occurring through geometrically highly oriented transition states; more oriented for the benzyl–phenyl coupling than for the phenyl–phenyl one, as a consequence of the higher directionality of the sp 3 orbital of the benzyl group in relation to the phenyl sp 2 orbital. The combination of both factors gives rise to a C(sp 3)–C(sp 2) reductive coupling faster than the C(sp 2)–C(sp 2) bond formation. Although a most demanding orientation requirement is needed for the C(sp 3)–C(sp 2)

Scheme 6. Reactions of 11a and 11b



coupling than for the $C(sp^2)-C(sp^2)$ bond formation, the energetic effort for the pregeneration of the $C(sp^3)-C(sp^2)$ bond is smaller. These observations represent an inversion for the pair $C(sp^2)-C(sp^2):C(sp^3)-C(sp^2)$ in the order $C(sp^2)-C(sp^2) > C(sp^3)-C(sp^2) > C(sp^3)-C(sp^3)$, theoretically established for the reductive elimination preference.^{14b,c} Previously, notable inversions had been observed for the pair $C(sp^3)-C(sp^2):C(sp^3)-C(sp^3)$ in competitive experiments.^{13a,e,37}

$$\ln \frac{[M]}{[M]_0} = -k_R t \quad (5)$$

Reductive Elimination of Fluorobenzene and Deprotonation of the Isomeric Mixture. The activation barrier for the intramolecular reductive elimination of fluorobenzene in **11a** and **11b** is not significantly different from the activation barrier for the C–H bond oxidative addition in **I**, since in solution hydride-rhodium(III)-aryl isomers are in equilibrium with spectroscopically nondetected amounts of their precursor intermediate. This is strongly supported by the reactions of the isomeric mixture with internal alkynes such as 2-butyne and 1-phenyl-1-propyne (Scheme 6). Such hydrocarbons do not undergo the insertion of the C–C triple bond into the Rh–H bond of the rhodium(III) isomers but provoke the displacement of fluorobenzene, to form the π -alkyne derivatives $[\text{Rh}(\eta^2\text{-MeC}\equiv\text{CR})\{\kappa^3\text{-P,O,P-}[\text{xant}(\text{P}^i\text{Pr}_2)_2]\}\text{BF}_4$ (R = Me (**13**), Ph (**14**)). These compounds were isolated as yellow solids in almost quantitative yield. Their $^{31}\text{P}\{^1\text{H}\}$ and $^{13}\text{C}\{^1\text{H}\}$ NMR spectra (Figures S64–S68) in acetone- d_6 reveal that the triple bond of the alkynes lies in a perpendicular plane to the P–Rh–P direction, in agreement with the X-ray structure previously reported for the related cation $[\text{Rh}(\eta^2\text{-PhC}\equiv\text{CPh})\{\kappa^3\text{-P,O,P-}[\text{xant}(\text{PPh}_2)_2]\}]^+$.^{18e} Thus, the $^{31}\text{P}\{^1\text{H}\}$ spectra show doublets ($^1J_{\text{P-Rh}} \approx 124$ Hz) at about 35 ppm, for the equivalent P^iPr_2 groups, whereas the $^{13}\text{C}\{^1\text{H}\}$ spectra display doublets ($^1J_{\text{C-Rh}} \approx 16$ Hz) of triplets ($^2J_{\text{C-P}} \approx 4$ Hz) for the C(sp)–carbon atoms, at 56.3 ppm for **13** and at 72.8 (CMe) and 61.2 (CPh) ppm for **14**.

The hydride ligand of **11a** and **11b** is fairly acidic, in agreement with the last step of the cycle shown in Scheme 1. Thus, the addition of 1.0 equiv of KO^tBu to acetone solutions of the isomeric mixture produces the abstraction of the hydride ligand and the formation of the corresponding mixture of the previously reported square-planar rhodium(I)-aryl derivatives $\text{Rh}(\sigma\text{-C}_6\text{H}_4\text{F})\{\kappa^3\text{-P,O,P-}[\text{xant}(\text{P}^i\text{Pr}_2)_2]\}$ (**15a**) and $\text{Rh}(m\text{-C}_6\text{H}_4\text{F})\{\kappa^3\text{-P,O,P-}[\text{xant}(\text{P}^i\text{Pr}_2)_2]\}$ (**15b**).^{10g,i} The reduction is

reversible, and the addition of 1.0 equiv of HBF₄·OEt₂ to fluorobenzene solutions of the rhodium(I) isomeric mixture regenerates the rhodium(III) one.

CONCLUDING REMARKS

This study has revealed that the oxidative addition of organic chlorides to the square-planar rhodium(I)-phenyl complex $\text{RhPh}\{\kappa^3\text{-P,O,P-}[\text{xant}(\text{P}^i\text{Pr}_2)_2]\}$ in the majority of the cases involves a cis addition of the C–Cl bond. Only for some particular organic chlorides, such as dichloromethane, the trans addition is competitive. The formation of the resulting rhodium(III) species is kinetically controlled by the C–Cl bond dissociation energy.

The coordinatively saturated compounds generated from the oxidative additions are stable toward a subsequent C–C reductive elimination. The abstraction of the chloride from the metal center gives rise to unsaturated five-coordinate species, displaying square pyramidal structures with the coordinated C-donor ligands at basal and axial positions. In contrast to the six-coordinate precursors, these compounds undergo C–C reductive coupling, with some noticeable exceptions as complexes bearing 2-pyridyl and methylchloride. The former backs to stabilize the metal center by coordination of the nitrogen atom, whereas the second one has the ability to promote the decomposition of the complex by means of the decarbonylation of solvents such as acetone. The activation energy of the reductive elimination depends upon the formed C–C bond. Thus, the $C(sp^3)-C(sp^2)$ reductive couplings are faster than the $C(sp^2)-C(sp^2)$ bond formation. In spite of that a most demanding orientation requirement is needed for the $C(sp^3)-C(sp^2)$ coupling than for the $C(sp^2)-C(sp^2)$ bond formation, the energetic effort for the pregeneration of the $C(sp^3)-C(sp^2)$ bond is smaller. In fluorobenzene, the reductive coupling is followed by a fast oxidative addition of a C–H bond of the solvent, which generates a fairly acidic hydride-rhodium(III)-aryl derivative. The deprotonation of the latter affords a new square planar rhodium(I)-aryl complex.

The reactions performed in this study starting from a square-planar rhodium(I)-aryl complex include C–Cl oxidative addition of organic chlorides, halide abstraction from the resulting six-coordinate rhodium(III) derivative, C–C reductive coupling between the initial aryl ligand and the added organic group, oxidative addition of a C–H bond of a new arene, and deprotonation of the generated hydride-rhodium(III)-aryl species to form a new square planar rhodium(I)-aryl derivative. They constitute a cycle of stoichiometric elemental

reactions, which defines the direct arylation promoted by a redox-pair Rh(I)–Rh(III). The results obtained suggest that the key steps of such arylation should be the C–Cl oxidative addition and the C–C reductive elimination. From a kinetic point of view, the former is controlled by the dissociation energy of the added bond, while the second one is governed by the dissociation energy of the formed bond. The weakest C–Cl bond is added faster, while the weakest C–C bond is also formed faster.

EXPERIMENTAL SECTION

General Information. All reactions were carried out with exclusion of air using Schlenk-tube techniques or in a glovebox. Instrumental methods and X-ray details are given in the [Supporting Information](#). In the NMR spectra (Figures S31–S68), the chemical shifts (in ppm) are referenced to residual solvent peaks (^1H , $^{13}\text{C}\{^1\text{H}\}$) or external 85% H_3PO_4 ($^{31}\text{P}\{^1\text{H}\}$), while J and N ($N = J_{\text{P-H}} + J_{\text{P-H}}$ for ^1H and $N = J_{\text{P-C}} + J_{\text{P-C}}$ for $^{13}\text{C}\{^1\text{H}\}$) are given in hertz. $\text{RhPh}\{\kappa^3\text{-P,O,P-[xant(P}^i\text{Pr}_2)_2]\}$ (**1**)^{10g} and $\text{RhCl}\{\kappa^3\text{-P,O,P-[xant(P}^i\text{Pr}_2)_2]\}$ (**2**)^{21a} were prepared by the published methods.

Reaction of $\text{RhPh}\{\kappa^3\text{-P,O,P-[xant(P}^i\text{Pr}_2)_2]\}$ (1**) with 2-Chloropyridine: Preparation of $\text{Rh(Ph)(2-pyridyl)Cl}\{\kappa^3\text{-P,O,P-[xant(P}^i\text{Pr}_2)_2]\}$ (**2**).** A solution of **1** (123 mg, 0.20 mmol) in 2-chloropyridine (3 mL) was stirred at 50 °C during 48 h. The resulting solution was evaporated to dryness to afford a yellowish residue. The addition of pentane (4 mL) afforded a white solid that was washed with pentane (2 × 2 mL) and dried in vacuo. Yield: 81 mg (56%). Anal. Calcd for $\text{C}_{38}\text{H}_{49}\text{ClNOP}_2\text{Rh}$: C, 62.00; H, 6.71; N, 1.90. Found: C, 62.22; H, 6.42; N, 2.16. HRMS (electrospray, m/z): calcd for $\text{C}_{38}\text{H}_{49}\text{NOP}_2\text{Rh}[\text{M} - \text{Cl}]^+$, 700.2339; found, 700.2342. IR (cm^{-1}): $\nu(\text{C}=\text{N})$ 1562 (m), $\nu(\text{C}-\text{O}-\text{C})$ 1192 (m). ^1H NMR (300.13 MHz, C_6D_6 , 298 K): δ 8.54 (d, $^3J_{\text{H-H}} = 2.8$, 1H, py), 8.44 (d, $^3J_{\text{H-H}} = 7.9$, 1H, py), 8.33 (d, $^3J_{\text{H-H}} = 7.4$, 1H, Ph), 7.31–6.59 (m, 11H, 3H Ph + 2H py + 6H CH-arom POP), 6.38 (t, $^3J_{\text{H-H}} = 7.0$, 1H, Ph), 3.46 (m, 2H, $\text{PCH}(\text{CH}_3)_2$), 2.63 (m, 2H, $\text{PCH}(\text{CH}_3)_2$), 1.48 (s, 3H, CH_3), 1.40–1.14 (m, 15H, 12H $\text{PCH}(\text{CH}_3)_2$ + 3H CH_3), 1.02 (dvt, $^3J_{\text{H-H}} = 7.3$, $N = 14.7$, 6H, $\text{PCH}(\text{CH}_3)_2$), 0.46 (dvt, $^3J_{\text{H-H}} = 6.8$, $N = 13.8$, 6H, $\text{PCH}(\text{CH}_3)_2$). $^{13}\text{C}\{^1\text{H}\}$ -apt NMR (75.48 MHz, C_6D_6 , 298 K): δ 173.9 (dt, $^1J_{\text{C-Rh}} = 40$, $^2J_{\text{C-P}} = 6$, Rh–C py), 154.2 (vt, $N = 12$, C-arom POP), 146.0 (s, CH py), 143.7 (dt, $^1J_{\text{C-Rh}} = 34$, $^2J_{\text{C-P}} = 10$, Rh–C Ph), 141.6 (s, CH Ph), 136.8 (t, $^3J_{\text{C-P}} = 4$, CH py), 136.4 (s, CH Ph), 133.5 (s, CH-arom POP), 132.0 (vt, $N = 5$, C-arom POP), 130.9 (s, CH py), 128.1 (s, CH-arom POP), 127.9 (s, CH Ph), 125.7 (s, CH Ph), 124.4 (s, CH-arom POP), 123.8 (vt, $N = 24.1$, C-arom POP), 122.8 (s, CH Ph), 117.5 (s, CH py), 35.3 (s, $\text{C}(\text{CH}_3)_2$), 34.7 (s, $\text{C}(\text{CH}_3)_2$), 28.6 (s, $\text{C}(\text{CH}_3)_2$), 27.6 (vt, $N = 21$, $\text{PCH}(\text{CH}_3)_2$), 25.6 (dvt, $N = 22$, $^2J_{\text{C-Rh}} = 2.0$, $\text{PCH}(\text{CH}_3)_2$), 21.7, 21.3, 20.0, 19.7 (all s, $\text{PCH}(\text{CH}_3)_2$). $^{31}\text{P}\{^1\text{H}\}$ NMR (121.49 MHz, C_6D_6 , 298 K): δ 27.7 (d, $^1J_{\text{Rh-P}} = 119$).

Reaction of $\text{RhPh}\{\kappa^3\text{-P,O,P-[xant(P}^i\text{Pr}_2)_2]\}$ (1**) with Chlorobenzene: Preparation of $\text{RhPh}_2\text{Cl}\{\kappa^3\text{-P,O,P-[xant(P}^i\text{Pr}_2)_2]\}$ (**3**).** A solution of **1** (100 mg, 0.16 mmol) in chlorobenzene (3 mL) was stirred at 90 °C during 48 h. The resulting solution was evaporated to dryness to afford a yellow residue. The addition of pentane (4 mL) afforded a yellowish white solid that was washed with pentane (2 × 2 mL) and dried in vacuo. Yield: 89.5 mg (76%). Anal. Calcd for $\text{C}_{39}\text{H}_{50}\text{ClOP}_2\text{Rh}$: C, 63.72; H, 6.86. Found: C, 63.35; H, 7.06. HRMS (electrospray, m/z): calcd for $\text{C}_{39}\text{H}_{50}\text{OP}_2\text{Rh}[\text{M} - \text{Cl}]^+$, 699.2392; found, 699.2397. IR (cm^{-1}): $\nu(\text{C}-\text{O}-\text{C})$ 1187 (m). ^1H NMR (400.16 MHz, C_6D_6 , 298 K): δ 8.55 (d, $^3J_{\text{H-H}} = 7.9$, 2H, Ph), 8.25 (d, $^3J_{\text{H-H}} = 7.1$, 1H, Ph), 7.30–7.02 (m, 9H, 4H CH-arom POP + 5H Ph), 6.94–6.83 (m, 3H, 2H CH-arom POP + 1H Ph), 6.68 (dt, $^3J_{\text{H-H}} = 1.4$, $^3J_{\text{H-H}} = 7.6$, 1H, Ph), 3.47 (m, 2H, $\text{PCH}(\text{CH}_3)_2$), 2.49 (m, 2H, $\text{PCH}(\text{CH}_3)_2$), 1.39 (dvt, $^3J_{\text{H-H}} = 7.3$, $N = 14.9$, 6H, $\text{PCH}(\text{CH}_3)_2$), 1.33 (s, 3H, CH_3), 1.23 (s, 3H, CH_3), 1.18 (dvt, $^3J_{\text{H-H}} = 7.3$, $N = 14.9$, 6H, $\text{PCH}(\text{CH}_3)_2$), 0.66 (dvt, $^3J_{\text{H-H}} = 6.9$, $N = 13.3$, 6H, $\text{PCH}(\text{CH}_3)_2$), 0.60 (dvt, $^3J_{\text{H-H}} = 7.0$, $N = 14.2$, 6H, $\text{PCH}(\text{CH}_3)_2$). $^{13}\text{C}\{^1\text{H}\}$ -apt NMR (75.48 MHz, C_6D_6 , 298 K): δ

155.4 (vt, $N = 11$, C-arom POP), 152.7 (dt, $^1J_{\text{C-Rh}} = 33$, $^2J_{\text{C-P}} = 8$, Rh–C Ph), 146.4 (dt, $^1J_{\text{C-Rh}} = 39$, $^3J_{\text{C-P}} = 9$, Rh–C Ph), 144.5, 142.5, 137.6 (all s, CH Ph), 133.2 (s, CH-arom POP), 132.7 (vt, $N = 5$, C-arom POP), 127.9 (s, CH-arom POP), 127.6, 125.7, 125.1 (all s, CH Ph), 124.3 (s, C-arom POP), 124.0 (s, CH-arom POP), 122.6 (s, CH Ph), 34.8 (s, $\text{C}(\text{CH}_3)_2$), 33.7, 27.8 (both s, $\text{C}(\text{CH}_3)_2$), 26.8 (vt, $N = 21.7$, $\text{PCH}(\text{CH}_3)_2$), 25.7 (vt, $N = 18$, $\text{PCH}(\text{CH}_3)_2$), 21.3, 20.4, 19.9, 19.6 (all s, $\text{PCH}(\text{CH}_3)_2$). $^{31}\text{P}\{^1\text{H}\}$ NMR (161.99 MHz, C_6D_6 , 298 K): δ 26.5 (d, $^1J_{\text{P-Rh}} = 114$).

Reaction of $\text{RhPh}\{\kappa^3\text{-P,O,P-[xant(P}^i\text{Pr}_2)_2]\}$ (1**) with Benzyl Chloride: Preparation of $\text{RhPh}(\text{CH}_2\text{Ph})\text{Cl}\{\kappa^3\text{-P,O,P-[xant(P}^i\text{Pr}_2)_2]\}$ (**4**).** A solution of **1** (105 mg, 0.17 mmol) in toluene (3 mL) was treated with benzyl chloride (19 μL , 0.17 mmol) and the resulting solution was stirred at room temperature for 5 min. After this time, it was evaporated to dryness to afford a yellowish residue. The addition of pentane (4 mL) afforded a white solid that was washed with pentane (2 × 2 mL) and dried in vacuo. Yield: 101 mg (80%). Anal. Calcd for $\text{C}_{40}\text{H}_{52}\text{ClOP}_2\text{Rh}$: C, 64.13; H, 7.00. Found: C, 63.75; H, 7.12. HRMS (electrospray, m/z): calcd for $\text{C}_{40}\text{H}_{52}\text{OP}_2\text{Rh}[\text{M} - \text{Cl}]^+$, 713.2543; found, 713.2557. IR (cm^{-1}): $\nu(\text{C}-\text{O}-\text{C})$ 1192 (m). ^1H NMR (300.13 MHz, C_6D_6 , 298 K): δ 8.67–8.45 (m, 3H, 1H Ph + 2H CH_2Ph), 7.34–6.74 (m, 11H, 2H Ph + 3H CH_2Ph + 6H CH-arom POP), 6.66 (d, $^3J_{\text{H-H}} = 7.4$, 1H, Ph), 6.36 (t, $^3J_{\text{H-H}} = 7.3$, 1H, Ph), 5.02 (dt, $^2J_{\text{H-Rh}} = 3.2$, $^3J_{\text{H-P}} = 3.6$, 2H, RhCH_2Ph), 3.39 (m, 2H, $\text{PCH}(\text{CH}_3)_2$), 2.22 (m, 2H, $\text{PCH}(\text{CH}_3)_2$), 1.44 (s, 3H, CH_3), 1.26 (dvt, $^3J_{\text{H-H}} = 7.1$, $N = 13.3$, 6H, $\text{PCH}(\text{CH}_3)_2$), 1.20 (s, 3H, CH_3), 1.17 (dvt, $^3J_{\text{H-H}} = 6.2$, $N = 13.0$, 6H, $\text{PCH}(\text{CH}_3)_2$), 0.85 (dvt, $^3J_{\text{H-H}} = 7.5$, $N = 15.0$, 6H, $\text{PCH}(\text{CH}_3)_2$), 0.13 (dvt, $^3J_{\text{H-H}} = 6.8$, $N = 13.3$, 6H, $\text{PCH}(\text{CH}_3)_2$). $^{13}\text{C}\{^1\text{H}\}$ -apt NMR (75.48 MHz, C_6D_6 , 298 K): δ 155.1 (t, $^3J_{\text{C-P}} = 4$, C CH_2Ph), 153.8 (vt, $N = 10.5$, C-arom POP), 141.9 (dt, $^1J_{\text{C-Rh}} = 33$, $^2J_{\text{C-P}} = 11$, Rh–C Ph), 140.4 (s, CH Ph), 137.4 (s, CH Ph), 133.2 (s, CH-arom POP), 132.0 (s, C-arom POP), 131.0 (s, CH CH_2Ph), 128.1 (s, CH CH_2Ph), 127.9 (s, CH-arom POP), 127.5 (s, CH Ph), 126.1 (s, CH Ph), 125.0 (s, CH CH_2Ph), 124.2 (s, CH-arom POP), 123.4 (vt, $N = 25.2$, C-arom POP), 122.7 (s, CH Ph), 34.9 (s, $\text{C}(\text{CH}_3)_2$), 34.6 (s, $\text{C}(\text{CH}_3)_2$), 28.5 (s, $\text{C}(\text{CH}_3)_2$), 27.1 (vt, $N = 19.2$, $\text{PCH}(\text{CH}_3)_2$), 26.2 (vt, $N = 19.7$, $\text{PCH}(\text{CH}_3)_2$), 22.9, 20.4, 19.5, 18.2 (all s, $\text{PCH}(\text{CH}_3)_2$), 16.8 (dt, $^1J_{\text{C-Rh}} = 29$, $^2J_{\text{C-P}} = 5$, Rh– CH_2Ph). $^{31}\text{P}\{^1\text{H}\}$ NMR (121.49 MHz, C_6D_6 , 298 K): δ 22.4 (d, $^1J_{\text{Rh-P}} = 118$).

Reaction of $\text{RhPh}\{\kappa^3\text{-P,O,P-[xant(P}^i\text{Pr}_2)_2]\}$ (1**) with Dichloromethane: Preparation of $\text{RhPh}(\text{CH}_2\text{Cl})\text{Cl}\{\kappa^3\text{-P,O,P-[xant(P}^i\text{Pr}_2)_2]\}$ (**5a–5b**).** Complex **1** (70 mg, 0.11 mmol) was dissolved in dichloromethane (3 mL), and the solution was stirred for 5 min at room temperature. The solution was evaporated to dryness to afford a yellow residue. The addition of pentane (4 mL) afforded a whitish solid that was washed with pentane (2 × 2 mL) and dried in vacuo. Yield: 55 mg (69%). Anal. Calcd for $\text{C}_{34}\text{H}_{47}\text{Cl}_2\text{OP}_2\text{Rh}$: C, 57.72; H, 6.70. Found: C, 57.31; H, 6.95. HRMS (electrospray, m/z): calcd for $\text{C}_{34}\text{H}_{47}\text{ClOP}_2\text{Rh}[\text{M} - \text{Cl}]^+$, 671.1846; found, 671.1855. IR (cm^{-1}): $\nu(\text{C}=\text{C})$ 1568 (w), $\nu(\text{C}-\text{O}-\text{C})$ 1196 (m). ^1H and $^{31}\text{P}\{^1\text{H}\}$ NMR spectra show the formation of **5a** and **5b** in a 1.1:1 ratio. ^1H NMR both isomers (300.13 MHz, CD_2Cl_2 , 298 K): δ 7.89 (d, $^3J_{\text{H-H}} = 7.6$, 1H, Ph), 7.74 (d, $^3J_{\text{H-H}} = 6.6$, 2H, Ph), 7.69–7.18 (m, 12H, CH-arom POP), 7.07 (t, $^3J_{\text{H-H}} = 7.6$, 1H, Ph), 6.92–6.80 (m, 3H, Ph), 6.72 (t, $^3J_{\text{H-H}} = 7.0$, 1H, Ph), 6.53 (d, $^3J_{\text{H-H}} = 8.0$, 1H, Ph), 6.38 (t, $^3J_{\text{H-H}} = 7.1$, 1H, Ph), 5.76 (dt, $^2J_{\text{H-Rh}} = 3.2$, $^3J_{\text{H-P}} = 6.5$, 2H, RhCH_2Cl), 4.79 (dt, $^2J_{\text{H-Rh}} = 2.0$, $^3J_{\text{H-P}} = 7.6$, 2H, RhCH_2Cl), 3.56, 3.25, 2.88, 2.50 (all m, 2H each, $\text{PCH}(\text{CH}_3)_2$), 1.82, 1.81, 1.62, 1.50 (all s, 3H each, CH_3), 1.47–1.34 (m, 12H, $\text{PCH}(\text{CH}_3)_2$), 1.30–1.12 (m, 24H, $\text{PCH}(\text{CH}_3)_2$), 0.93 (dvt, $^3J_{\text{H-H}} = 7.3$, $N = 14.6$, 6H, $\text{PCH}(\text{CH}_3)_2$), 0.38 (dvt, $^3J_{\text{H-H}} = 7.2$, $N = 14.1$, 6H, $\text{PCH}(\text{CH}_3)_2$). $^{13}\text{C}\{^1\text{H}\}$ -apt NMR both isomers (75.48 MHz, CD_2Cl_2 , 298 K): δ 154.1 (vt, $N = 12.7$, C-arom POP), 153.6 (vt, $N = 11.9$, C-arom POP), 142.3 (dt, $^1J_{\text{C-Rh}} = 34$, $^2J_{\text{C-P}} = 10$, Rh–C Ph), 140.4 (dt, $^1J_{\text{C-Rh}} = 37$, $^2J_{\text{C-P}} = 10$, Rh–C Ph), 138.6, 137.7, 136.2 (all s, CH Ph), 134.3 (s, CH-arom POP), 134.2 (s, CH-arom POP), 132.3 (vt, $N = 6$, C-arom POP), 132.2 (vt, $N = 4$, C-arom POP), 129.7, 129.6 (both s, CH-arom POP), 128.4 (s, CH Ph), 126.4 (s, CH Ph), 124.9 (vt, $N = 5$, CH-arom POP), 124.0 (vt, $N = 5$, CH-arom POP), 123.3 (vt, $N = 22$, C-

arom POP), 123.0 (s, CH Ph), 122.9 (vt, $N = 19$, C-arom POP), 122.4 (s, CH Ph), 40.7 (dt, $^1J_{C-Rh} = 34$, $^2J_{C-P} = 8$, Rh-CH₂Cl), 40.2 (dt, $^1J_{C-Rh} = 37$, $^2J_{C-P} = 6$, Rh-CH₂Cl), 36.6 (s, C(CH₃)₂), 35.1 (s, C(CH₃)₂), 34.8, 32.2, 30.6 (all s, C(CH₃)₂), 28.2 (vt, $N = 22.7$, PCH(CH₃)₂), 26.6 (vt, $N = 24$, PCH(CH₃)₂), 26.0 (vt, $N = 21$, PCH(CH₃)₂), 25.0 (vt, $N = 19$, PCH(CH₃)₂), 21.8, 21.7, 21.2, 21.0, 20.6, 19.7, 19.6, 19.5 (all s, PCH(CH₃)₂). $^{31}P\{^1H\}$ NMR both isomers (161.99 MHz, CD₂Cl₂, 298 K): δ 27.5 (d, $^1J_{Rh-P} = 114$), 27.3 (d, $^1J_{Rh-P} = 110$).

Kinetic Analysis of the Reaction of 1 with 2-Chloropyridine. In the glovebox, an NMR tube was charged with a solution of **1** (20 mg, 0.03 mmol) in 2-chloropyridine (0.5 mL), and a capillary tube filled with a solution of the internal standard (PCy₃) in toluene-*d*₈ was placed in the NMR tube. The tube was immediately introduced into an NMR probe preheated at the desired temperature (323, 328, 333, 338, and 343 K), and the reaction was monitored by $^{31}P\{^1H\}$ NMR spectroscopy (a delay of 25 s was used) at different intervals of time. The experiments were performed in duplicate. Rate constants were obtained by plotting eq 1. Errors were calculated using the standard deviation data provided by Microsoft Excel.

Kinetic Analysis of the Reaction of 1 with Chlorobenzene. In the glovebox, an NMR tube was charged with a solution of **1** (20 mg, 0.03 mmol) in chlorobenzene (0.5 mL), and a capillary tube filled with a solution of the internal standard (PCy₃) in toluene-*d*₈ was placed in the NMR tube. The tube was immediately introduced into an NMR probe preheated at the desired temperature (363, 373, 383, 393, and 398 K), and the reaction was monitored by $^{31}P\{^1H\}$ NMR spectroscopy (a delay of 25 s was used) at different intervals of time. The experiments were performed in duplicate. Rate constants were obtained by plotting eq 1. Errors were calculated using the standard deviation data provided by Microsoft Excel.

Kinetic Analysis of the Reaction of 1 with Dichloromethane. In the glovebox, an NMR tube was charged with a solution of **1** (20 mg, 0.03 mmol) and dichloromethane (41 μ L, 0.64 mmol) in toluene-*d*₈ (0.5 mL), and a capillary tube filled with a solution of the internal standard (PCy₃) in toluene-*d*₈ was placed in the NMR tube. The tube was immediately introduced into an NMR probe at the desired temperature (268, 273, 278, 288, and 298 K), and the reaction was monitored by $^{31}P\{^1H\}$ NMR spectroscopy (a delay of 25 s was used) at different intervals of time. The experiments were performed in duplicate. Rate constants were calculated using the standard deviation data provided by Microsoft Excel.

Reaction of Rh(Ph)(2-pyridyl)Cl(κ^3 -P,O,P-[xant(PⁱPr)₂]) (2) with NaBF₄: Preparation of [RhPh(η^2 -C,N-(NC₅H₄))(κ^3 -P,O,P-[xant(PⁱPr)₂])]BF₄ (6). A solution of **2** (100 mg, 0.13 mmol) in acetone (3 mL) was treated with NaBF₄ (15 mg, 0.13 mmol), and the resulting mixture was stirred at room temperature for 1 h. After this time, it was evaporated to dryness to afford a light brown residue and methylene chloride (4 mL) was added. The resulting suspension was filtered through Celite to remove the sodium salts and the solution obtained was evaporated to dryness to afford a yellow residue. The addition of diethyl ether (4 mL) afforded a white solid that was washed with diethyl ether (2 \times 2 mL) and dried in vacuo. Yield: 96 mg (90%). Anal. Calcd for C₃₈H₄₉BF₄NOP₂Rh: C, 57.96; H, 6.27; N, 1.78. Found: C, 57.57; H, 6.41; N, 1.73. HRMS (electrospray, m/z): calcd for C₃₈H₄₉NOP₂Rh [M]⁺, 700.2339; found, 700.2315. IR (cm⁻¹): ν (C=N) 1551 (m), ν (C-O-C) 1189 (m), ν (B-F) 1055 (vs). 1H NMR (400.13 MHz, CD₂Cl₂, 233 K): δ 8.30 (d, $^3J_{H-H} = 4.5$, 1H, py), 8.19 (d, $^3J_{H-H} = 7.9$, 1H, py), 8.09 (d, $^3J_{H-H} = 7.7$, 1H, Ph), 7.87 (d, $^3J_{H-H} = 7.1$, 2H, CH-arom POP), 7.73 (t, $^3J_{H-H} = 7.2$, 1H, py), 7.48 (t, $^3J_{H-H} = 7.6$, 2H, CH-arom POP), 7.32 (m, 2H, CH-arom POP), 7.01 (m, 2H, 1H py + 1H Ph), 6.75 (t, $^3J_{H-H} = 7.1$, 1H, Ph), 6.37 (t, $^3J_{H-H} = 7.1$, 1H, Ph), 5.70 (d, $^3J_{H-H} = 7.9$, 1H, Ph), 2.64 (m, 2H, PCH(CH₃)₂), 2.01 (s, 3H, CH₃), 1.69 (m, 2H, PCH(CH₃)₂), 1.51 (s, 3H, CH₃), 1.06–0.95 (m, 12H, PCH(CH₃)₂), 0.91 (dvt, $^3J_{H-H} = 7.6$, $N = 15.9$, 6H, PCH(CH₃)₂), -0.04 (dvt, $^3J_{H-H} = 7.8$, $N = 15.3$, 6H, PCH(CH₃)₂). $^{13}C\{^1H\}$ -apt NMR (100.62 MHz, CD₂Cl₂, 233 K): δ 158.0 (dt, $^1J_{C-Rh} = 34$, $^2J_{C-P} = 8$, Rh-C py), 154.3 (vt, $N = 11$, C-arom POP), 142.2 (s, CH py), 139.4 (s, CH Ph), 138.6 (s, CH

py), 135.4 (dt, $^1J_{C-Rh} = 44$, $^2J_{C-P} = 9$, Rh-C Ph), 132.5 (s, CH-arom POP), 132.4 (s, C-arom POP), 132.3 (s, CH Ph), 130.5 (s, CH-arom POP), 127.9 (s, CH Ph), 127.8 (s, CH Ph), 126.8 (s, CH-arom POP), 123.9 (s, CH Ph), 122.5 (s, CH py), 119.5 (s, CH py), 116.7 (vt, $N = 30$, C-arom POP), 36.2 (s, C(CH₃)₂), 34.8 (s, C(CH₃)₂), 27.1 (s, C(CH₃)₂), 25.3 (vt, $N = 22$, PCH(CH₃)₂), 23.7 (vt, $N = 26$, PCH(CH₃)₂), 18.4, 16.2, 16.1 (all s, PCH(CH₃)₂), 16.8 (vt, $N = 8$, PCH(CH₃)₂). $^{31}P\{^1H\}$ NMR (161.98 MHz, CD₂Cl₂, 233 K): δ 37.2 (d, $^1J_{Rh-P} = 113$). $^{19}F\{^1H\}$ NMR (282.38 MHz, CD₂Cl₂, 298 K): δ -153.5 (s, BF₄).

Reaction of RhPh₂Cl(κ^3 -P,O,P-[xant(PⁱPr)₂]) (3) with AgBF₄: Preparation of [RhPh₂(κ^3 -P,O,P-[xant(PⁱPr)₂])]BF₄ (7). A solution of **3** (100 mg, 0.14 mmol) in acetone (3 mL) was treated with AgBF₄ (27 mg, 0.14 mmol), and the resulting mixture was stirred at room temperature in the absence of light for 1 h. After this time, it was filtered through Celite to remove the silver salts and was evaporated to dryness to afford a yellow residue. The addition of diethyl ether (4 mL) afforded a yellow solid that was washed with diethyl ether (2 \times 2 mL) and dried in vacuo. Yield: 102 mg (95%). Anal. Calcd for C₃₉H₅₀BF₄OP₂Rh: C, 59.56; H, 6.41. Found: C, 59.12; H, 6.43. HRMS (electrospray, m/z): calcd for C₃₉H₅₀OP₂Rh [M]⁺, 699.2386; found, 699.2379. IR (cm⁻¹): ν (C-O-C) 1183 (m), ν (B-F) 1053 (vs). 1H NMR (300.13 MHz, CD₂Cl₂, 298 K): δ 7.97 (dd, $^3J_{H-H} = 7.5$, $^3J_{H-H} = 1.3$, 2H, CH-arom POP), 7.71–7.47 (m, 4H, CH-arom POP), 7.36 (br, 4H, Ph), 7.01 (m, 6H, Ph), 2.73 (m, 4H, PCH(CH₃)₂), 1.88 (s, 6H, CH₃), 0.95 (dvt, $^3J_{H-H} = 7.4$, $N = 16.6$, 12H, PCH(CH₃)₂), 0.81 (dvt, $^3J_{H-H} = 6.7$, $N = 14.2$, 12H, PCH(CH₃)₂). $^{13}C\{^1H\}$ -apt NMR (75.48 MHz, CD₂Cl₂, 298 K): δ 153.4 (vt, $N = 9.3$, C-arom POP), 141.7 (dt, $^1J_{C-Rh} = 41$, $^2J_{C-P} = 8$, Rh-C Ph), 133.1 (s, CH-arom POP), 132.8 (s, C-arom POP, inferred from the HMBC spectrum), 132.5 (s, CH Ph), 131.4 (s, CH-arom POP), 127.9 (s, CH Ph), 127.0 (s, CH-arom POP), 124.7 (s, CH Ph), 117.4 (vt, $N = 28.4$, C-arom POP), 34.6 (s, C(CH₃)₂), 32.8 (s, C(CH₃)₂), 24.8 (vt, $N = 23$, PCH(CH₃)₂), 18.0, 17.1 (both s, PCH(CH₃)₂). $^{13}C\{^1H\}$ -apt NMR (100.62, CD₂Cl₂, 183 K): δ 152.7 (vt, $N = 9$, C-arom POP), 146.6 (broad doublet, $^1J_{C-Rh} = 42$, Rh-C Ph), 138.7 (broad doublet, $^1J_{C-Rh} = 44$, Rh-C Ph), 138.2 (s, CH Ph), 132.8 (s, CH-arom POP), 131.5 (s, C-arom POP), 131.4 (s, CH-arom POP), 128.5 (s, CH Ph), 128.2 (s, CH Ph), 127.4 (s, CH Ph), 126.8 (s, CH Ph), 126.5 (s, CH-arom POP), 124.2 (s, CH Ph), 123.6 (s, CH Ph), 116.1 (vt, $N = 29$, C-arom POP), 35.3 (s, C(CH₃)₂), 34.1 (s, C(CH₃)₂), 29.8 (s, C(CH₃)₂), 25.2 (vt, $N = 29$, PCH(CH₃)₂), 22.6 (vt, $N = 22$, PCH(CH₃)₂), 18.4, 16.4 (both s, PCH(CH₃)₂). $^{31}P\{^1H\}$ NMR (121.50 MHz, CD₂Cl₂, 298 K): δ 31.2 (d, $^1J_{P-Rh} = 119$). $^{19}F\{^1H\}$ NMR (282.38 MHz, CD₂Cl₂, 298 K): δ -153.3 (s, BF₄).

Reaction of RhPh(CH₂Ph)Cl(κ^3 -P,O,P-[xant(PⁱPr)₂]) (4) with AgBF₄: Preparation of [RhPh(CH₂Ph)(κ^3 -P,O,P-[xant(PⁱPr)₂])]BF₄ (8). A solution of **4** (100 mg, 0.13 mmol) in acetone (3 mL) was treated with AgBF₄ (27 mg, 0.14 mmol), and the resulting mixture was stirred at room temperature in the absence of light for 1 h. After this time, the mixture was filtered through Celite to remove the silver salts and the solution obtained was evaporated to dryness to afford a yellow residue. The addition of diethyl ether (4 mL) afforded a yellow solid that was washed with diethyl ether (2 \times 2 mL) and dried in vacuo. Yield: 105 mg (98%). Anal. Calcd for C₄₀H₅₂BF₄OP₂Rh: C, 60.01; H, 6.55. Found: C, 59.64; H, 6.77. HRMS (electrospray, m/z): calcd for C₄₀H₅₂OP₂Rh [M]⁺, 713.2543; found, 713.2555. IR (cm⁻¹): ν (C-O-C) 1183 (m), ν (B-F) 1053 (vs). 1H NMR (300.13 MHz, CD₂Cl₂, 233 K): δ 7.83 (d, $^3J_{H-H} = 7.4$, 2H, CH-arom POP), 7.71 (d, $^3J_{H-H} = 7.3$, 2H, CH₂Ph), 7.58–7.19 (m, 8H, 4 CH-arom POP + 1H Ph + 3H CH₂Ph), 6.95 (t, $^3J_{H-H} = 8.1$, 1H, Ph), 6.71 (t, $^3J_{H-H} = 7.1$, 1H, Ph), 6.15 (t, $^3J_{H-H} = 7.7$, 1H, Ph), 5.50 (d, $^3J_{H-H} = 8.4$, 1H, Ph), 4.82 (m, 2H, Rh-CH₂Ph), 2.89 (m, 2H, PCH(CH₃)₂), 2.66 (m, 2H, PCH(CH₃)₂), 2.03 (s, 3H, CH₃), 1.56 (dvt, $^3J_{H-H} = 8.47$, $N = 16.6$, 6H, PCH(CH₃)₂), 1.24 (s, 3H, CH₃), 0.97 (dvt, $^3J_{H-H} = 5.9$, $N = 11.9$, 6H, PCH(CH₃)₂), 0.31 (dvt, $^3J_{H-H} = 8.0$, $N = 16.4$, 6H, PCH(CH₃)₂), 0.04 (dvt, $^3J_{H-H} = 7.4$, $N = 15.1$, 6H, PCH(CH₃)₂). $^{13}C\{^1H\}$ -apt NMR (75.48 MHz, CD₂Cl₂, 233 K): δ 155.2 (s, C-arom POP), 141.5 (s, C CH₂Ph), 134.6 (s, CH Ph), 133.4 (s, C-arom

POP), 132.8 (s, CH-arom POP), 131.1 (dt, $^1J_{C-Rh} = 41$, $^2J_{C-P} = 8$, Rh–C Ph), 130.3 (s, CH CH₂Ph), 130.2 (s, CH Ph), 129.6 (s, CH CH₂Ph), 129.1 (s, CH-arom POP), 128.6 (s, CH Ph), 128.3 (s, CH CH₂Ph), 127.8 (s, CH Ph), 126.7 (s, CH-arom POP), 124.7 (s, CH Ph), 115.1 (vt, $N = 31$, C-arom POP), 35.0 (s, C(CH₃)₂), 34.6 (s, C(CH₃)₂), 26.9 (vt, $N = 20$, PCH(CH₃)₂), 23.5 (vt, $N = 23$, PCH(CH₃)₂), 23.1 (s, C(CH₃)₂), 22.6 (d, $^1J_{C-Rh} = 28$, Rh–CH₂Ph), 19.1, 17.6, 16.7, 16.1 (all s, PCH(CH₃)₂). $^{31}P\{^1H\}$ NMR (121.50 MHz, CD₂Cl₂, 298 K): δ 27.8 (d, $^1J_{P-Rh} = 121$). $^{19}F\{^1H\}$ NMR (282.38 MHz, CD₂Cl₂, 298 K): δ –153.5 (s, BF₄).

Reaction of RhPh(CH₂Cl)Cl(κ^3 -P,O,P-[xant(PⁱPr)₂]) (5a–5b) with AgBF₄. A solution of 5a–5b (100 mg, 0.14 mmol) in acetone (3 mL) was treated with AgBF₄ (28 mg, 0.14 mmol), and the resulting mixture was stirred at room temperature in the absence of light for 1 h. After this time, the mixture was filtered through Celite to remove the silver salts and the solution obtained was evaporated to dryness to afford a yellow residue. The addition of diethyl ether (4 mL) afforded a yellow solid. According to the 1H and $^{31}P\{^1H\}$ NMR spectra, the solid is a mixture from which [RhPh(CH₂Cl)(κ^3 -P,O,P-[xant(PⁱPr)₂])BF₄ (9) and [Rh(CO)(κ^3 -P,O,P-[xant(PⁱPr)₂])BF₄ (10, vide infra) were identified.

Spectroscopic Data of [RhPh(CH₂Cl)(κ^3 -P,O,P-[xant(PⁱPr)₂])BF₄ (9). HRMS (electrospray, m/z): calcd for C₃₄H₄₇CLOP₂Rh [M]⁺, 671.1840; found, 671.1868. 1H NMR (400.13 MHz, acetone-*d*₆, 243 K): δ 8.19 (d, $^3J_{H-H} = 7.6$, 2H, CH-arom POP), 7.82–7.63 (m, 4H, CH-arom POP), 7.29 (m, 1H, Ph), 6.98 (t, $^3J_{H-H} = 7.5$, 1H, Ph), 6.81 (t, $^3J_{H-H} = 7.7$, 1H, Ph), 6.41 (t, $^3J_{H-H} = 6.9$, 1H, Ph), 5.96 (m, 3H CH₂Cl + 1H Ph), 3.19 (m, 2H, PCH(CH₃)₂), 2.98 (m, 2H, PCH(CH₃)₂), 2.12 (s, 3H, CH₃), 1.58 (s, 3H, CH₃), 1.47 (dvt, $^3J_{H-H} = 8.7$, $N = 16.3$, 6H, PCH(CH₃)₂), 1.25 (dvt, $^3J_{H-H} = 6.2$, $N = 11.8$, 6H, PCH(CH₃)₂), 0.98 (dvt, $^3J_{H-H} = 7.8$, $N = 15.4$, 6H, PCH(CH₃)₂), 0.03 (dvt, $^3J_{H-H} = 7.6$, $N = 14.4$, 6H, PCH(CH₃)₂). $^{13}C\{^1H\}$ -apt NMR (100.62 MHz, acetone-*d*₆, 253 K): 155.1 (vt, $N = 11$, C-arom POP), 137.1 (s, CH Ph), 135.1 (dt, $^1J_{C-Rh} = 44$, $^2J_{C-P} = 9$, Rh–C Ph), 134.0 (s, CH-arom POP), 133.4 (vt, $N = 5$, C-arom POP), 132.1 (s, CH-arom POP), 130.7, 129.5, 128.7 (all s, CH Ph), 128.0 (vt, $N = 6$, CH-arom POP), 125.3 (s, CH-arom Ph), 116.5 (vt, $N = 31$, C-arom POP), 45.5 (dt, $^1J_{C-Rh} = 34$, $^2J_{C-P} = 7$, Rh–CH₂Cl), 36.1 (s, C(CH₃)₂), 35.3 (s, C(CH₃)₂), 27.5 (s, C(CH₃)₂), 26.4 (vt, $N = 21$, PCH(CH₃)₂), 24.4 (dvt, $^1J_{C-Rh} = 2$, $N = 26$, PCH(CH₃)₂), 20.0, 16.8, 16.6, 16.5 (all s, PCH(CH₃)₂). $^{31}P\{^1H\}$ NMR (161.98 MHz, acetone-*d*₆, 243 K): δ 31.2 (d, $^1J_{Rh-P} = 113$).

Preparation of [Rh(CO)(κ^3 -P,O,P-[xant(PⁱPr)₂])BF₄ (10). A solution of 5a–5b (94 mg, 0.13 mmol) in acetone (3 mL) was treated with AgBF₄ (26 mg, 0.13 mmol), and the resulting mixture was stirred at room temperature in the absence of light for 1 h. After this time, the mixture was filtered through Celite to remove the silver salts and the solution obtained was evaporated to dryness to afford a yellow residue. This residue was dissolved in acetone (3 mL), was stirred at 70 °C for 24 h, and was evaporated to dryness, and the addition of diethyl ether (4 mL) afforded a yellow solid that was washed with diethyl ether (2 × 2 mL) and dried in vacuo. Yield: 76 mg (87%). Anal. Calcd C₂₈H₄₀BF₄O₂P₂Rh: C, 50.93; H, 6.11. Found: C, 51.32; H, 6.32. HRMS (electrospray, m/z): calcd for C₂₈H₄₀O₂P₂Rh [M]⁺, 573.1553; found, 573.1621. IR (cm^{–1}): ν (CO) 1978 (s), ν (C–O–C) 1190 (m), ν (B–F) 1054 (vs). 1H NMR (300.13 MHz, acetone-*d*₆, 273 K): δ 8.07 (dd, $^3J_{H-H} = 7.8$, $^4J_{H-H} = 1.4$, 2H, CH-arom POP), 7.93 (m, 2H, CH-arom POP), 7.62 (t, $^3J_{H-H} = 7.6$, 2H, CH-arom POP), 3.00 (m, 4H, PCH(CH₃)₂), 1.78 (s, 6H, CH₃), 1.41 (dvt, $^3J_{H-H} = 11.8$, $N = 17.0$, 12H, PCH(CH₃)₂), 1.22 (dvt, $^3J_{H-H} = 9.9$, $N = 17.0$, 12H, PCH(CH₃)₂). $^{13}C\{^1H\}$ -apt NMR (75.48 MHz, acetone-*d*₆, 273 K): δ 191.5 (dt, $^1J_{C-Rh} = 86$, $^2J_{C-P} = 14$, Rh–CO), 156.7 (vt, $N = 16$, C-arom POP), 133.5 (s, CH-arom POP), 133.4 (s, CH-arom POP), 132.5 (vt, $N = 6$, C-arom POP), 128.2 (vt, $N = 6$, CH-arom POP), 118.4 (dvt, $^2J_{C-Rh} = 1$, $N = 29$, C-arom POP), 34.8 (vt, $N = 1$, C(CH₃)₂), 33.4 (s, C(CH₃)₂), 27.4 (dvt, $^1J_{C-Rh} = 2$, $N = 14$, PCH(CH₃)₂), 19.8 (vt, $N = 6.0$, PCH(CH₃)₂), 19.2 (s, PCH(CH₃)₂). $^{31}P\{^1H\}$ NMR (121.50 MHz, acetone-*d*₆, 273 K): δ 64.0 (d, $^1J_{Rh-P} = 114$).

Reaction of [RhPh(κ^3 -P,O,P-[xant(PⁱPr)₂])BF₄ (7) with Fluorobenzene. An NMR tube was charged with a solution of 7 (5 mg, 6.3 × 10^{–3} mmol) in fluorobenzene (2 mL) and it is introduced in an oil bath preheated at 80 °C, and it was periodically checked by $^{31}P\{^1H\}$ NMR spectroscopy. After 5 days, the $^{31}P\{^1H\}$ NMR spectrum showed quantitative conversion to RhH(*o*-C₆H₄F)(κ^1 -FBF₃)(κ^3 -P,O,P-[xant(PⁱPr)₂]) (11a) and RhH(*m*-C₆H₄F)(κ^1 -FBF₃)(κ^3 -P,O,P-[xant(PⁱPr)₂]) (11b), while the GC–MS spectrum showed the formation of biphenyl.

Reaction of [RhPh(CH₂Ph)(κ^3 -P,O,P-[xant(PⁱPr)₂])BF₄ (8) with Fluorobenzene. An NMR tube was charged with a solution of 8 (5 mg, 6.2 × 10^{–3} mmol) in fluorobenzene (2 mL) and it is introduced in an oil bath preheated at 80 °C. $^{31}P\{^1H\}$ NMR spectra were recorded periodically and after 2 days showed quantitative conversion to RhH(*o*-C₆H₄F)(κ^1 -FBF₃)(κ^3 -P,O,P-[xant(PⁱPr)₂]) (11a) and RhH(*m*-C₆H₄F)(κ^1 -FBF₃)(κ^3 -P,O,P-[xant(PⁱPr)₂]) (11b), while in the 1H NMR spectrum, a singlet at 4.00 ppm, assigned to benzylbenzene,³⁸ is observed.

Kinetic Analysis of the Reaction of 7 with Fluorobenzene. In the glovebox, an NMR tube was charged with a solution of 7 (5 mg, 6.3 × 10^{–3} mmol) in fluorobenzene (2 mL), and a capillary tube filled with a solution of the internal standard (PCy₃) in toluene-*d*₈ was placed in the NMR tube. The tube was introduced into a thermostatic bath at 343, 348, 353, 358, or 363 K and the reaction was monitored by $^{31}P\{^1H\}$ NMR spectroscopy (a delay of 25 s was used) at different intervals of time. The experiments were performed in duplicate. Rate constants were obtained by plotting eq 5. Errors were calculated using the standard deviation data provided by Microsoft Excel.

Kinetic Analysis of the Reaction of 8 with Fluorobenzene. In the glovebox, an NMR tube was charged with a solution of 8 (5 mg, 6.2 × 10^{–3} mmol) in fluorobenzene (2 mL), and a capillary tube filled with a solution of the internal standard (PCy₃) in toluene-*d*₈ was placed in the NMR tube. The tube was introduced into a thermostatic bath at 338, 353, 358, or 363 K and the reaction was monitored by $^{31}P\{^1H\}$ NMR spectroscopy (a delay of 25 s was used) at different intervals of time. The experiments were performed in duplicate. Rate constants were obtained by plotting eq 5. Errors were calculated using the standard deviation data provided by Microsoft Excel.

Reaction of RhCl(κ^3 -P,O,P-[xant(PⁱPr)₂]) (12) with AgBF₄ in Fluorobenzene: Preparation of RhH(*o*-C₆H₄F)(κ^1 -FBF₃)(κ^3 -P,O,P-[xant(PⁱPr)₂]) (11a) and RhH(*m*-C₆H₄F)(κ^1 -FBF₃)(κ^3 -P,O,P-[xant(PⁱPr)₂]) (11b). A solution of 12 (100 mg, 0.17 mmol) in fluorobenzene (3 mL) was treated with AgBF₄ (34 mg, 0.17 mmol), and the resulting mixture was stirred at room temperature in the absence of light for 1 h. After this time, the mixture was filtered through Celite to remove the silver salts and the solution obtained was evaporated to dryness to afford a light yellow residue. The addition of diethyl ether (4 mL) afforded a yellow solid that was washed with diethyl ether (2 × 2 mL) and dried in vacuo. Yield: 67 mg (53%). The $^{31}P\{^1H\}$ NMR spectra in acetone-*d*₆ show the formation of an isomeric mixture of RhH(*o*-C₆H₄F)(κ^1 -FBF₃)(κ^3 -P,O,P-[xant(PⁱPr)₂]) (11a) and RhH(*m*-C₆H₄F)(κ^1 -FBF₃)(κ^3 -P,O,P-[xant(PⁱPr)₂]) (11b) in a ratio 70:30. Anal. Calcd for C₃₃H₄₅BF₃O₂P₂Rh: C, 54.41; H, 6.23. Found: C, 54.39; H, 6.25. HRMS (electrospray, m/z): calcd for C₃₃H₄₅FOP₂Rh [M]⁺, 641.1979; found, 641.1986. IR (cm^{–1}): ν (C–O–C) 1188 (m), ν (B–F) 1095 (s), 953 (s), 745 (s).

NMR Data for RhH(*o*-C₆H₄F)(κ^1 -FBF₃)(κ^3 -P,O,P-[xant(PⁱPr)₂]) (11a). 1H NMR (400.13 MHz, acetone-*d*₆, 273 K): δ 8.08 (br, 1H, C₆H₄-2-F), 8.01 (dd, $^3J_{H-H} = 7.8$, $^4J_{H-H} = 1.3$, 2H, CH-arom POP), 7.80 (m, 2H, CH-arom POP), 7.50 (t, $^3J_{H-H} = 7.6$, 2H, CH-arom POP), 6.96 (m, 2H, C₆H₄-2-F), 6.83 (t, $^3J_{H-H} = 8.6$, 1H, C₆H₄-2-F), 3.00 (m, 2H, PCH(CH₃)₂), 2.68 (m, 2H, PCH(CH₃)₂), 1.77 (s, 3H, CH₃), 1.76 (s, 3H, CH₃), 1.17 (dvt, $^3J_{H-H} = 7.5$, $N = 14.4$, 6H, PCH(CH₃)₂), 1.08 (dvt, $^3J_{H-H} = 7.2$, $N = 14.4$, 6H, PCH(CH₃)₂), 1.01 (dvt, $^3J_{H-H} = 9.3$, $N = 16.5$, 6H, PCH(CH₃)₂), 0.86 (dvt, $^3J_{H-H} = 9.5$, $N = 16.5$, 6H, PCH(CH₃)₂), –18.95 (dt, $^1J_{H-Rh} = 30.6$, $^2J_{H-H} = 12.9$, 1H, Rh–H). $^{13}C\{^1H\}$ -apt NMR (100.63 MHz, acetone-*d*₆, 273 K): δ 166.2 (broad d, $^1J_{C-F} = 230$, C–F C₆H₄F), 154.3 (vt, $N = 13$, C-arom POP), 145.7 (broad d, $^1J_{C-Rh} = 34$, Rh–C C₆H₄F), 136.3

(broad d, $J_{C-F} = 10$, CH C_6H_4F), 132.8 (s, CH-arom POP), 132.6 (s, CH-arom POP), 132.3 (dvt, $J_{C-Rh} = 3$, $N = 20$, C-arom POP), 127.2 (vt, $N = 6$, CH arom POP), 124.9 (d, $J_{C-F} = 8$, CH C_6H_4F), 123.6 (s, CH C_6H_4F), 120.4 (vt, $N = 28$, C-arom POP), 114.3 (d, $J_{C-F} = 30$, CH, C_6H_4F), 34.9 (s, $C(CH_3)_2$), 34.4, 33.2 (both s, $C(CH_3)_2$), 27.9 (vt, $N = 29$, $PCH(CH_3)_2$), 26.2 (vt, $N = 23$, $PCH(CH_3)_2$), 19.0, 17.6 (both s, $PCH(CH_3)_2$), 17.5 (vt, $N = 5$, $PCH(CH_3)_2$). $^{31}P\{^1H\}$ NMR (121.4 MHz, acetone- d_6 , 298 K): δ 43.6 (d, $^1J_{Rh-P} = 111.0$). $^{19}F\{^1H\}$ NMR (376.46 MHz, acetone- d_6 , 273 K): δ -88.3 (d, $J_{F-Rh} = 21.7$, C_6H_4F), -151.4 (s, BF_4).

Characteristic NMR Data for $RhH(m-C_6H_4F)(\kappa^1-FBF_3)(\kappa^3-P,O,P-[xant(P^iPr_2)_2])$ (11b). 1H NMR (400.13 MHz, acetone- d_6 , 273 K): δ -19.92 (dt, $^1J_{H-Rh} = 35.5$, $^2J_{H-P} = 13.4$, 1H, Rh-H). $^{31}P\{^1H\}$ NMR (121.4 MHz, acetone- d_6 , 298 K): δ 40.9 (d, $^1J_{Rh-P} = 115$). $^{19}F\{^1H\}$ NMR (376.46 MHz, acetone- d_6 , 273 K): δ -115.7 (s, C_6H_4F), -151.4 (s, BF_4).

Reaction of $RhH(o-C_6H_4F)(\kappa^1-FBF_3)(\kappa^3-P,O,P-[xant(P^iPr_2)_2])$ (11a) and $RhH(m-C_6H_4F)(\kappa^1-FBF_3)(\kappa^3-P,O,P-[xant(P^iPr_2)_2])$ (11b) with 2-Butyne: Preparation of $[Rh(\eta^2-MeC\equiv CMe)(\kappa^3-P,O,P-[xant(P^iPr_2)_2])][BF_4]$ (13). A solution of 11a–11b (80 mg, 0.11 mmol) in fluorobenzene (3 mL) was treated with 2-butyne (9 μ L, 0.11 mmol) and the resulting mixture was stirred at room temperature for 24 h. After this time, the solution was evaporated to dryness to afford a yellow residue. The addition of diethyl ether (4 mL) afforded a yellow solid that was washed with diethyl ether (2 \times 2 mL) and dried in vacuo. Yield: 75 mg (98%). Anal. Calcd for $C_{31}H_{46}BF_4OP_2Rh$: C, 54.25; H, 6.76. Found: C, 54.17; H, 6.89. HRMS (electrospray, m/z): calcd for $C_{31}H_{46}OP_2Rh [M]^+$, 599.2073; found, 599.2048. IR (cm^{-1}): $\nu(C\equiv C)$ 1994 (w), $\nu(C-O-C)$ 1187 (m), $\nu(B-F)$ 1051 (vs). 1H NMR (300.13 MHz, acetone- d_6 , 298 K): δ 7.96 (dd, $^2J_{H-H} = 7.7$, $^3J_{H-H} = 1.4$, 2H, CH-arom POP), 7.67 (m, 2H, CH-arom POP), 7.51 (t, $^3J_{H-H} = 15.2$, 2H, CH-arom POP), 2.70 (m, 4H, $PCH(CH_3)_2$), 2.34 (d, $^3J_{H-Rh} = 1.9$, 6H, $\equiv CCH_3$), 1.77 (s, 6H, CH_3), 1.33 (dvt, $^3J_{H-H} = 9.4$, $N = 16.8$, 12H, $PCH(CH_3)_2$), 1.25 (dvt, $^3J_{H-H} = 7.5$, $N = 14.7$, 12H, $PCH(CH_3)_2$). $^{13}C\{^1H\}$ -apt NMR (75.48 MHz, acetone- d_6 , 298 K): δ 156.9 (vt, $N = 14$, C-arom POP), 133.0 (s, CH-arom POP), 132.8 (s, CH-arom POP), 132.0 (vt, $N = 5$, C-arom POP), 127.4 (vt, $N = 5$, CH-arom POP), 119.1 (vt, $N = 24$, C-arom POP), 56.3 (dt, $^1J_{C-Rh} = 16$, $^2J_{C-P} = 3$, $\equiv CCH_3$), 34.8 (s, $C(CH_3)_2$), 33.9 (s, $C(CH_3)_2$), 25.0 (vt, $N = 22$, $PCH(CH_3)_2$), 18.4 (vt, $N = 6$, $PCH(CH_3)_2$), 10.1 (d, $^2J_{C-Rh} = 1$, $\equiv CCH_3$). $^{31}P\{^1H\}$ NMR (121.49 MHz, acetone- d_6 , 298 K): δ 35.4 (d, $^1J_{Rh-P} = 125$). $^{19}F\{^1H\}$ NMR (282.38 MHz, acetone- d_6 , 298 K): δ -151.8 (s, BF_4).

Reaction of $RhH(o-C_6H_4F)(\kappa^1-FBF_3)(\kappa^3-P,O,P-[xant(P^iPr_2)_2])$ (11a) and $RhH(m-C_6H_4F)(\kappa^1-FBF_3)(\kappa^3-P,O,P-[xant(P^iPr_2)_2])$ (11b) with 1-Phenyl-1-propyne: Preparation of $[Rh(\eta^2-PhC\equiv CMe)(\kappa^3-P,O,P-[xant(P^iPr_2)_2])][BF_4]$ (14). A solution of 11a–11b (80 mg, 0.11 mmol) in fluorobenzene (3 mL) was treated with 1-phenyl-1-propyne (14 μ L, 0.11 mmol), and the resulting mixture was stirred at room temperature for 24 h. After this time, the solution was evaporated to dryness to afford a yellow residue. The addition of diethyl ether (4 mL) afforded a yellow solid that was washed with diethyl ether (2 \times 2 mL) and dried in vacuo. Yield: 77 mg (94%). Anal. Calcd for $C_{36}H_{48}BF_4OP_2Rh$: C, 57.77; H, 6.46. Found: C, 57.70; H, 6.27. HRMS (electrospray, m/z): calcd for $C_{36}H_{48}OP_2Rh [M]^+$, 661.2230; found, 661.2237. IR (cm^{-1}): $\nu(C-O-C)$ 1186 (m), $\nu(B-F)$ 1051–1027 (vs). 1H NMR (300.13 MHz, acetone- d_6 , 298 K): δ 8.09 (dd, $^2J_{H-H} = 8.0$, $^3J_{H-H} = 1.6$, 2H, Ph), 8.01 (dd, $^2J_{H-H} = 7.7$, $^3J_{H-H} = 1.3$, 2H, CH-arom POP), 7.66 (m, 2H, CH-arom POP), 7.53 (t, $^3J_{H-H} = 15.2$, 2H, CH-arom POP), 7.50–7.38 (m, 3H, Ph), 2.80–2.60 (m, 5H, 3H $\equiv CCH_3$, 2H $PCH(CH_3)_2$), 2.48 (m, 2H, $PCH(CH_3)_2$), 1.81 (s, 3H, CH_3), 1.80 (s, 3H, CH_3), 1.37 (dvt, $^3J_{H-H} = 9.2$, $N = 17.0$, 6H, $PCH(CH_3)_2$), 1.26 (dvt, $^3J_{H-H} = 6.9$, $N = 13.8$, 6H, $PCH(CH_3)_2$), 1.06 (dvt, $^3J_{H-H} = 8.3$, $N = 15.7$, 6H, $PCH(CH_3)_2$), 1.02 (dvt, $^3J_{H-H} = 9.4$, $N = 16.6$, 6H, $PCH(CH_3)_2$). $^{13}C\{^1H\}$ -apt NMR (75.48 MHz, acetone- d_6 , 298 K): δ 156.8 (vt, $N = 13$, C-arom POP), 133.0 (s, CH-arom POP), 132.9 (s, CH-arom POP), 132.3 (d, $J_{Rh-C} = 2$, CH Ph), 132.1 (vt, $N = 5$, C-arom POP), 129.3 (s, CH Ph), 128.8 (s, CH Ph), 127.6 (vt, $N = 5$, CH-arom POP), 126.9 (s, C Ph), 119.0 (vt, $N = 25$, C-arom POP), 72.8 (dt, $^1J_{C-Rh} = 16$, $^2J_{C-P} = 5$, $\equiv CCH_3$), 61.2 (dt,

$^1J_{C-Rh} = 18$, $^2J_{C-P} = 3$, $PhC\equiv$), 34.9 (s, $C(CH_3)_2$), 34.1 (s, $C(CH_3)_2$), 33.7 (s, $C(CH_3)_2$), 25.5 (vt, $N = 21$, $PCH(CH_3)_2$), 24.4 (vt, $N = 23$, $PCH(CH_3)_2$), 19.0 (vt, $N = 6$, $PCH(CH_3)_2$), 18.1, 17.5 (both s, $PCH(CH_3)_2$), 17.7 (vt, $N = 6$, $PCH(CH_3)_2$), 11.5 (s, $\equiv CCH_3$). $^{31}P\{^1H\}$ NMR (121.49 MHz, acetone- d_6 , 298 K): δ 35.6 (d, $^1J_{Rh-P} = 122$). $^{19}F\{^1H\}$ NMR (282.38 MHz, acetone- d_6 , 298 K): δ -151.8 (s, BF_4).

Reaction of the Isomeric Mixture of 11a and 11b with K^tOBu . A solution of the isomeric mixture of 11a and 11b (32 mg, 0.044 mmol) in acetone was treated with K^tOBu (5 mg, 0.044 mmol), and the resulting mixture was stirred at room temperature for 1 h. After this time, the solution was evaporated to dryness, toluene was added, and the resulting suspension was filtered through Celite to remove the potassium salts. The solution obtained was evaporated to dryness to afford a red residue. $^{31}P\{^1H\}$ and $^{19}F\{^1H\}$ NMR spectroscopies show the quantitative formation of the previously reported $Rh(o-C_6H_4F)-\{\kappa^3-P,O,P-[xant(P^iPr_2)_2]\}$ (15a)^{10g} and $Rh(m-C_6H_4F)-\{\kappa^3-P,O,P-[xant(P^iPr_2)_2]\}$ (15b)¹⁰ⁱ a ratio 7:3. $^{31}P\{^1H\}$ NMR (121.49 MHz, benzene- d_6 , 298 K): δ 39.7 (d, $^1J_{Rh-P} = 168$, 15a), 37.1 (d, $^1J_{Rh-P} = 174$, 15b). $^{19}F\{^1H\}$ NMR (282.38 MHz, benzene- d_6 , 298 K): δ -85.4 (dt, $^3J_{Rh-F} = 19.8$, $^4J_{P-F} = 4$, 15a), -118.4 (s, 15b).

Protonation of the Isomeric Mixture of 15a and 15b with HBf_4 . A solution of the isomeric mixture of 15a and 15b (200 mg, 0.31 mmol) in fluorobenzene (3 mL) was treated with $HBf_4 \cdot OEt_2$ (43 μ L, 0.31 mmol), and the solution was stirred at room temperature for 1 h. After this time, it was evaporated to dryness to afford a light yellow residue. The addition of diethyl ether (4 mL) afforded a white solid that was washed with diethyl ether (2 \times 2 mL) and dried in vacuo. Yield: 189 mg (83%). The $^{31}P\{^1H\}$ NMR spectrum in acetone- d_6 showed the regeneration of the isomeric mixture of 11a and 11b.

ASSOCIATED CONTENT

Supporting Information

The Supporting Information is available free of charge at <https://pubs.acs.org/doi/10.1021/acs.organomet.1c00643>.

General information for the experimental section, kinetic plots, structural analysis, and NMR spectra (PDF)

Accession Codes

CCDC 2121578–2121584 contain the supplementary crystallographic data for this paper. These data can be obtained free of charge via www.ccdc.cam.ac.uk/data_request/cif, or by emailing data_request@ccdc.cam.ac.uk, or by contacting The Cambridge Crystallographic Data Centre, 12 Union Road, Cambridge CB2 1EZ, UK; fax: +44 1223 336033.

AUTHOR INFORMATION

Corresponding Author

Miguel A. Esteruelas – Departamento de Química Inorgánica—Instituto de Síntesis Química y Catálisis Homogénea (ISQCH)—Centro de Innovación en Química Avanzada (ORFEO-CINQA), Universidad de Zaragoza—CSIC, 50009 Zaragoza, Spain; orcid.org/0000-0002-4829-7590; Email: maester@unizar.es

Authors

Laura A. de las Heras – Departamento de Química Inorgánica—Instituto de Síntesis Química y Catálisis Homogénea (ISQCH)—Centro de Innovación en Química Avanzada (ORFEO-CINQA), Universidad de Zaragoza—CSIC, 50009 Zaragoza, Spain

Montserrat Oliván – Departamento de Química Inorgánica—Instituto de Síntesis Química y Catálisis Homogénea (ISQCH)—Centro de Innovación en Química Avanzada (ORFEO-CINQA), Universidad de Zaragoza—CSIC,

50009 Zaragoza, Spain; orcid.org/0000-0003-0381-0917

Enrique Oñate – Departamento de Química Inorgánica—Instituto de Síntesis Química y Catálisis Homogénea (ISQCH)—Centro de Innovación en Química Avanzada (ORFEO-CINQA), Universidad de Zaragoza—CSIC, 50009 Zaragoza, Spain; orcid.org/0000-0003-2094-719X

Complete contact information is available at:

<https://pubs.acs.org/10.1021/acs.organomet.1c00643>

Notes

The authors declare no competing financial interest.

ACKNOWLEDGMENTS

Financial support from the MICIN/AEI/10.13039/501100011033 (PID2020-115286GB-I00 and RED2018-102387-T), Gobierno de Aragón (E06_20R and LMP23_21), FEDER, and the European Social Fund is acknowledged. L.A.d.l.H. thanks the MECO for her FPU contract (FPU17/04813, “ESF investing in your future”).

REFERENCES

- (1) Corbet, J.-P.; Mignani, G. Selected Patented Cross-Coupling Reaction Technologies. *Chem. Rev.* **2006**, *106*, 2651–2710.
- (2) Ackermann, L.; Vicente, R.; Kapdi, A. R. Transition-Metal-Catalyzed Direct Arylation of (Hetero)Arenes by C-H Bond Cleavage. *Angew. Chem., Int. Ed.* **2009**, *48*, 9792–9826.
- (3) (a) Magano, J.; Dunetz, J. R. Large-Scale Applications of Transition Metal-Catalyzed Couplings for the Synthesis of Pharmaceuticals. *Chem. Rev.* **2011**, *111*, 2177–2250. (b) Len, C.; Bruniaux, S.; Delbecq, F.; Parmar, V. S. Palladium-Catalyzed Suzuki-Miyaura Cross-Coupling in Continuous Flow. *Catalysts* **2017**, *7*, 146. (c) Roy, D.; Uozumi, Y. Recent Advances in Palladium-Catalyzed Cross-Coupling Reactions at ppm to ppb Molar Catalyst Loadings. *Adv. Synth. Catal.* **2018**, *360*, 602–625. (d) Biffis, A.; Centomo, P.; Del Zotto, A.; Zecca, M. Pd Metal Catalysts for Cross-Couplings and Related Reactions in the 21st Century: A Critical Review. *Chem. Rev.* **2018**, *118*, 2249–2295. (e) Campeau, L.-C.; Hazari, N. Cross-Coupling and Related Reactions: Connecting Past Success to the Development of New Reactions for the Future. *Organometallics* **2019**, *38*, 3–35. (f) González-Sebastián, L.; Morales-Morales, D. Cross-coupling reactions catalysed by palladium pincer complexes. A review of recent advances. *J. Organomet. Chem.* **2019**, *893*, 39–51.
- (4) (a) Colby, D. A.; Bergman, R. G.; Ellman, J. A. Rhodium-Catalyzed C-C Bond Formation via Heteroatom-Directed C-H Bond Activation. *Chem. Rev.* **2010**, *110*, 624–655. (b) Bouffard, J.; Itami, K. Rhodium-Catalyzed C-H Bond Arylation of Arenes. *Top. Curr. Chem.* **2010**, *292*, 231–280. (c) Yang, Z.; Yu, J.-T.; Pan, C. Recent advances in rhodium-catalyzed C(sp²)-H (hetero)arylation. *Org. Biomol. Chem.* **2021**, *19*, 8442–8465.
- (5) (a) Takahashi, H.; Inagaki, S.; Nishihara, Y.; Shibata, T.; Takagi, K. Novel Rh Catalysis in Cross-Coupling between Alkyl Halides and Arylzinc Compounds Possessing ortho-COX (X = OR, NMe₂, or Ph) Groups. *Org. Lett.* **2006**, *8*, 3037–3040. (b) Takahashi, H.; Inagaki, S.; Yoshii, N.; Gao, F.; Nishihara, Y.; Takagi, K. Rh-Catalyzed Negishi Alkyl-Aryl Cross-Coupling Leading to α - or β -Phosphoryl-Substituted Alkylarenes. *J. Org. Chem.* **2009**, *74*, 2794–2797. (c) Ejiri, S.; Odo, S.; Takahashi, H.; Nishimura, Y.; Gotoh, K.; Nishihara, Y.; Takagi, K. Negishi Alkyl-Aryl Cross-Coupling Catalyzed by Rh: Efficiency of Novel Tripodal 3-Diphenylphosphino-2-(diphenylphosphino)methyl-2-methylpropyl Acetate Ligand. *Org. Lett.* **2010**, *12*, 1692–1695. (d) Sato, K.; Inoue, Y.; Mori, T.; Sakaue, A.; Tarui, A.; Omote, M.; Kumadaki, I.; Ando, A. Csp³-Csp³ Homocoupling Reaction of Benzyl Halides Catalyzed by Rhodium. *Org. Lett.* **2014**, *16*, 3756–3759.
- (6) Grushin, V. V.; Alper, H. Transformations of Chloroarenes, Catalyzed by Transition-Metal Complexes. *Chem. Rev.* **1994**, *94*, 1047–1062.
- (7) (a) Jones, W. D.; Feher, F. J. Comparative Reactivities of Hydrocarbon C-H Bonds with a Transition-Metal Complex. *Acc. Chem. Res.* **1989**, *22*, 91–100. (b) Shilov, A. E.; Shul'pin, G. B. Activation of C-H Bonds by Metal Complexes. *Chem. Rev.* **1997**, *97*, 2879–2932. (c) Eisenstein, O.; Milani, J.; Perutz, R. N. Selectivity of C-H Activation and Competition between C-H and C-F Bond Activation at Fluorocarbons. *Chem. Rev.* **2017**, *117*, 8710–8753. (d) Pabst, T. P.; Chirik, P. J. A Tutorial on Selectivity Determination in C(sp²)-H Oxidative Addition of Arenes by Transition Metal Complexes. *Organometallics* **2021**, *40*, 813–831.
- (8) Fagnou, K.; Lautens, M. Rhodium-Catalyzed Carbon-Carbon Bond Forming Reactions of Organometallic Compounds. *Chem. Rev.* **2003**, *103*, 169–196.
- (9) Saikia, I.; Borah, A. J.; Phukan, P. Use of Bromine and Bromo-Organic Compounds in Organic Synthesis. *Chem. Rev.* **2016**, *116*, 6837–7042.
- (10) (a) Darensbourg, D. J.; Groetsch, G.; Wiegrefe, P.; Rheingold, A. L. Insertion Reactions of Carbon Dioxide with Square-Planar Rhodium Alkyl and Aryl Complexes. *Inorg. Chem.* **1987**, *26*, 3827–3830. (b) Boyd, S. E.; Field, L. D.; Hambley, T. W.; Partridge, M. G. Synthesis and Characterization of Rh(P(CH₃)₃)₂(CO)CH₃ and Rh(P(CH₃)₃)₂(CO)Ph. *Organometallics* **1993**, *12*, 1720–1724. (c) Krug, C.; Hartwig, J. F. Direct Observation of Aldehyde Insertion into Rhodium-Aryl and -Alkoxide Complexes. *J. Am. Chem. Soc.* **2002**, *124*, 1674–1679. (d) Macgregor, S. A.; Roe, D. C.; Marshall, W. J.; Bloch, K. M.; Bakhmutov, V. I.; Grushin, V. V. The F/Ph Rearrangement Reaction of [(Ph₃P)₃RhF], the Fluoride Congener of Wilkinson's Catalyst. *J. Am. Chem. Soc.* **2005**, *127*, 15304–15321. (e) Sun, Z.-M.; Zhao, P. Rhodium-Mediated Decarboxylative Conjugate Addition of Fluorinated Benzoic Acids: Stoichiometric and Catalytic Transformations. *Angew. Chem., Int. Ed.* **2009**, *48*, 6726–6730. (f) Truscott, B. J.; Fortman, G. C.; Slawin, A. M. Z.; Nolan, S. P. Well-defined [Rh(NHC)(OH)] complexes enabling the conjugate addition of arylboronic acids to α,β -unsaturated ketones. *Org. Biomol. Chem.* **2011**, *9*, 7038–7041. (g) Esteruelas, M. A.; Oliván, M.; Vélez, A. POP-Rhodium-Promoted C-H and B-H Bond Activation and C-B-Bond Formation. *Organometallics* **2015**, *34*, 1911–1924. (h) Esteruelas, M. A.; Oliván, M.; Vélez, A. Conclusive Evidence on the Mechanism of the Rhodium-Mediated Decyanative Borylation. *J. Am. Chem. Soc.* **2015**, *137*, 12321–12329. (i) Curto, S. G.; Esteruelas, M. A.; Oliván, M.; Oñate, E.; Vélez, A. Selective C-Cl Bond Oxidative Addition of Chloroarenes to a POP-Rhodium Complex. *Organometallics* **2017**, *36*, 114–128. (j) Adams, G. M.; Colebatch, A. L.; Skornia, J. T.; McKay, A. I.; Johnson, H. C.; Lloyd-Jones, G. C.; Macgregor, S. A.; Beattie, N. A.; Weller, A. S. Dehydropolymerization of H₃B-NMe₂ To Form Polyaminoboranes Using [Rh(Xantphos-alkyl)] Catalysts. *J. Am. Chem. Soc.* **2018**, *140*, 1481–1495.
- (11) (a) Gatard, S.; Çelenligil-Çetin, R.; Guo, C.; Foxman, B. M.; Ozerov, O. V. Carbon-Halide Oxidative Addition and Carbon-Carbon Reductive Elimination at a (PNP)Rh Center. *J. Am. Chem. Soc.* **2006**, *128*, 2808–2809. (b) Gatard, S.; Guo, C.; Foxman, B. M.; Ozerov, O. V. Thioether, Dinitrogen, and Olefin Complexes of (PNP)Rh: Kinetics and Thermodynamics of Exchange and Oxidative Addition Reactions. *Organometallics* **2007**, *26*, 6066–6075. (c) Ito, J.-i.; Miyakawa, T.; Nishiyama, H. Amine-Assisted C-Cl Bond Activation of Aryl Chlorides by a (Phebox)Rh-Chloro Complex. *Organometallics* **2008**, *27*, 3312–3315. (d) Douglas, T. M.; Chaplin, A. B.; Weller, A. S. Dihydrogen Loss from a 14-Electron Rhodium(III) Bis-Phosphine Dihydride To Give a Rhodium(I) Complex That Undergoes Oxidative Addition with Aryl Chlorides. *Organometallics* **2008**, *27*, 2918–2921. (e) Chen, S.; Li, Y.; Zhao, J.; Li, X. Chelation-Assisted Carbon-Halogen Bond Activation by a Rhodium(I) Complex. *Inorg. Chem.* **2009**, *48*, 1198–1206. (f) Wu, H.; Hall, M. B. Kinetic C-H Oxidative Addition vs Thermodynamic C-X Oxidative Addition of Chlorobenzene by a Neutral Rh(I) System. A Density Functional

- Theory Study. *J. Phys. Chem. A* **2009**, *113*, 11706–11712. (g) Puri, M.; Gatard, S.; Smith, D. A.; Ozerov, O. V. Competition Studies of Oxidative Addition of Aryl Halides to the (PNP)Rh Fragment. *Organometallics* **2011**, *30*, 2472–2482. (h) Qian, Y. Y.; Lee, M. H.; Yang, W.; Chan, K. S. Aryl carbon-chlorine (Ar-Cl) and aryl carbon-fluorine (Ar-F) bond cleavages by rhodium porphyrins. *J. Organomet. Chem.* **2015**, *791*, 82–89. (i) König, A.; Fischer, C.; Alberico, E.; Selle, C.; Drexler, H.-J.; Baumann, W.; Heller, D. Oxidative Addition of Aryl Halides to Cationic Bis(phosphane)rhodium Complexes: Application in C-C Bond Formation. *Eur. J. Inorg. Chem.* **2017**, *2017*, 2040–2047.
- (12) (a) Tejel, C.; Ciriano, M. A.; López, J. A.; Jiménez, S.; Bordonaba, M.; Oro, L. A. One-Electron versus Two-Electron Mechanisms in the Oxidative Addition Reactions of Chloroalkanes to Amido-Bridged Rhodium Complexes. *Chem.—Eur. J.* **2007**, *13*, 2044–2053. (b) Blank, B.; Glatz, G.; Kempe, R. Single and Double C-Cl-Activation of Methylene Chloride by P,N-ligand Coordinated Rhodium Complexes. *Chem.—Asian J.* **2009**, *4*, 321–327. (c) Vetter, A. J.; Rieth, R. D.; Brennessel, W. W.; Jones, W. D. Selective C-H Activation of Haloalkanes using a Rhodiumtrispyrazolylborate Complex. *J. Am. Chem. Soc.* **2009**, *131*, 10742–10752. (d) Ho, H.-A.; Dunne, J. F.; Ellern, A.; Sadow, A. D. Reactions of Tris(oxazolonyl)phenylborato Rhodium(I) with C-X (X = Cl, Br, OTf) Bonds: Stereoselective Intermolecular Oxidative Addition. *Organometallics* **2010**, *29*, 4105–4114. (e) Adams, G. M.; Chadwick, F. M.; Pike, S. D.; Weller, A. S. A CH₂Cl₂ complex of a [Rh(pincer)]⁺ cation. *Dalton Trans.* **2015**, *44*, 6340–6342. (f) Jiao, Y.; Brennessel, W. W.; Jones, W. D. Oxidative Addition of Chlorohydrocarbons to a Rhodium Tris(pyrazolyl)borate Complex. *Organometallics* **2015**, *34*, 1552–1566. (g) Curto, S. G.; de las Heras, L. A.; Esteruelas, M. A.; Oliván, M.; Oñate, E. C(sp³)-Cl Bond Activation Promoted by a POP-Pincer Rhodium(I) Complex. *Organometallics* **2019**, *38*, 3074–3083.
- (13) (a) Madison, B. L.; Thyme, S. B.; Keene, S.; Williams, B. S. Mechanistic Study of Competitive sp³-sp³ and sp²-sp³ Carbon-Carbon Reductive Elimination from a Platinum (IV) Center and the Isolation of a C-C Agostic Complex. *J. Am. Chem. Soc.* **2007**, *129*, 9538–9539. (b) Luedtke, A. T.; Goldberg, K. I. Reductive Elimination of Ethane from Five-Coordinate Platinum(IV) Alkyl Complexes. *Inorg. Chem.* **2007**, *46*, 8496–8498. (c) Zucca, A.; Maidich, L.; Canu, L.; Petretto, G. L.; Stoccoro, S.; Cinellu, M. A.; Clarkson, G. J.; Rourke, J. P. Rollover-Assisted C(sp²)-C(sp³) Bond Formation. *Chem.—Eur. J.* **2014**, *20*, 5501–5510. (d) Chen, S.; Su, Y.; Han, K.; Li, X. Mechanistic studies on C-C reductive coupling of five-coordinate Rh(III) complexes. *Org. Chem. Front.* **2015**, *2*, 783–791. (e) Bowes, E. G.; Pal, S.; Love, J. A. Exclusive Csp³-Csp³ vs Csp²-Csp³ Reductive Elimination from Pt^{IV} Governed by Ligand Constraints. *J. Am. Chem. Soc.* **2015**, *137*, 16004–16007.
- (14) (a) Tatsumi, K.; Hoffmann, R.; Yamamoto, A.; Stille, J. K. Reductive Elimination of d⁸-Organotransition Metal Complexes. *Bull. Chem. Soc. Jpn.* **1981**, *54*, 1857–1867. (b) Ananikov, V. P.; Musaev, D. G.; Morokuma, K. Theoretical Insight into the C-C Coupling Reactions of the Vinyl, Phenyl, Ethynyl, and Methyl Complexes of Palladium and Platinum. *Organometallics* **2005**, *24*, 715–723. (c) Ananikov, V. P.; Musaev, D. G.; Morokuma, K. Critical Effect of Phosphane Ligands on the Mechanism of Carbon-Carbon Bond Formation Involving Palladium(II) Complexes: A Theoretical Investigation of Reductive Elimination from Square-Planar and T-Shaped Species. *Eur. J. Inorg. Chem.* **2007**, *2007*, 5390–5399. (d) Puddephatt, R. J. Selectivity in carbon-carbon coupling reactions at palladium(IV) and platinum(IV). *Can. J. Chem.* **2019**, *97*, 529–537.
- (15) (a) Shaw, P. A.; Clarkson, G. J.; Rourke, J. P. Long-Lived Five-Coordinate Platinum(IV) Intermediates: Regiospecific C-C Coupling. *Organometallics* **2016**, *35*, 3751–3762. (b) Shaw, P. A.; Rourke, J. P. Selective C-C coupling at a Pt(IV) centre: 100% preference for sp²-sp³ over sp³-sp³. *Dalton Trans.* **2017**, *46*, 4768–4776.
- (16) (a) Fekl, U.; Kaminsky, W.; Goldberg, K. I. A Stable Five-Coordinate Platinum(IV) Alkyl Complex. *J. Am. Chem. Soc.* **2001**, *123*, 6423–6424. (b) Sangtrirutnugul, P.; Stradiotto, M.; Tilley, T. D. Rhodium Complexes Containing a Tridentate Bis(8-quinolyl)-methylsilyl Ligand: Synthesis and Reactivity. *Organometallics* **2006**, *25*, 1607–1617. (c) Ghosh, R.; Zhang, X.; Achord, P.; Emge, T. J.; Krogh-Jespersen, K.; Goldman, A. S. Dimerization of Alkynes Promoted by a Pincer-Ligated Iridium Complex. C-C Reductive Elimination Inhibited by Steric Crowding. *J. Am. Chem. Soc.* **2007**, *129*, 853–866. (d) Zhao, S.-B.; Wu, G.; Wang, S. Steric Impact of Neutral N,N-Chelates on the Structure and Stability of Five-Coordinate Platinum(IV) Complexes: fac-Pt^{IV}Me₃ Complexes of BAB and BAM. *Organometallics* **2008**, *27*, 1030–1033. (e) Ghosh, R.; Emge, T. J.; Krogh-Jespersen, K.; Goldman, A. S. Combined Experimental and Computational Studies on Carbon-Carbon Reductive Elimination from Bis(hydrocarbyl) Complexes of (PCP)Ir. *J. Am. Chem. Soc.* **2008**, *130*, 11317–11327. (f) Tan, R.; Song, D. Interconversion between the Enantiomers of Chiral Five-Coordinate Me₃Pt(IV) Complexes. *Inorg. Chem.* **2011**, *50*, 10614–10622. (g) Timpa, S. D.; Fafard, C. M.; Herbert, D. E.; Ozerov, O. V. Catalysis of Kumada-Tamao-Corriu coupling by a (POCOP)Rh pincer complex. *Dalton Trans.* **2011**, *40*, 5426–5429. (h) Zhu, Y.; Smith, D. A.; Herbert, D. E.; Gatard, S.; Ozerov, O. V. C-H and C-O oxidative addition in reactions of aryl carboxylates with a PNP pincer-ligated Rh(I) fragment. *Chem. Commun.* **2012**, *48*, 218–220. (i) Scheuermann, M. L.; Luedtke, A. T.; Hanson, S. K.; Fekl, U.; Kaminsky, W.; Goldberg, K. I. Reactions of Five-Coordinate Platinum(IV) Complexes with Molecular Oxygen. *Organometallics* **2013**, *32*, 4752–4758.
- (17) Morris, R. H. Brønsted-Lowry Acid Strength of Metal Hydride and Dihydrogen Complexes. *Chem. Rev.* **2016**, *116*, 8588–8654.
- (18) (a) Pawley, R. J.; Moxham, G. L.; Dallanegra, R.; Chaplin, A. B.; Brayshaw, S. K.; Weller, A. S.; Willis, M. C. Controlling Selectivity in Intermolecular Alkene or Aldehyde Hydroacylation Reactions Catalyzed by [Rh(L₂)]⁺ Fragments. *Organometallics* **2010**, *29*, 1717–1728. (b) Pontiggia, A. J.; Chaplin, A. B.; Weller, A. S. Cationic iridium complexes of the Xantphos ligand. Flexible coordination modes and the isolation of the hydride insertion product with an alkene. *J. Organomet. Chem.* **2011**, *696*, 2870–2876. (c) Dallanegra, R.; Chaplin, A. B.; Weller, A. S. Rhodium Cyclopentyl Phosphine Complexes of Wide-Bite-Angle Ligands DPEphos and Xantphos. *Organometallics* **2012**, *31*, 2720–2728. (d) Johnson, H. C.; Leitao, E. M.; Whittell, G. R.; Manners, I.; Lloyd-Jones, G. C.; Weller, A. S. Mechanistic Studies of the Dehydrocoupling and Dehydropolymerization of Amine-Boranes Using a [Rh(Xantphos)]⁺ Catalyst. *J. Am. Chem. Soc.* **2014**, *136*, 9078–9093. (e) Ren, P.; Pike, S. D.; Pernik, I.; Weller, A. S.; Willis, M. C. Rh-POP Pincer Xantphos Complexes for C-S and C-H Activation. Implications for Carbothiolation Catalysis. *Organometallics* **2015**, *34*, 711–723. (f) Barwick-Silk, J.; Hardy, S.; Willis, M. C.; Weller, A. S. Rh(DPEphos)-Catalyzed Alkyne Hydroacylation Using β-Carbonyl-Substituted Aldehydes: Mechanistic Insight Leads to Low Catalyst Loadings that Enables Selective Catalysis on Gram-Scale. *J. Am. Chem. Soc.* **2018**, *140*, 7347–7357. (g) Adams, G. M.; Ryan, D. E.; Beattie, N. A.; McKay, A. I.; Lloyd-Jones, G. C.; Weller, A. S. Dehydropolymerization of H₃B-NMeH₂ Using a [Rh(DPEphos)]⁺ Catalyst: The Promoting Effect of NMeH₂. *ACS Catal.* **2019**, *9*, 3657–3666. (h) Dietz, M.; Johnson, A.; Martínez-Martínez, A.; Weller, A. S. The [Rh(Xantphos)]⁺ catalyzed hydroboration of diphenylacetylene using trimethylamine-borane. *Inorg. Chim. Acta* **2019**, *491*, 9–13. (i) Ryan, D. E.; Andrea, K. A.; Race, J. J.; Boyd, T. M.; Lloyd-Jones, G. C.; Weller, A. S. Amine-Borane Dehydropolymerization Using Rh-Based Precatalysts: Resting State, Chain Control, and Efficient Polymer Synthesis. *ACS Catal.* **2020**, *10*, 7443–7448.
- (19) Asensio, G.; Cuenca, A. B.; Esteruelas, M. A.; Medio-Simón, M.; Oliván, M.; Valencia, M. Osmium(III) Complexes with POP Pincer Ligands: Preparation from Commercially Available OsCl₃·3H₂O and Their X-ray Structures. *Inorg. Chem.* **2010**, *49*, 8665–8667.
- (20) (a) Alós, J.; Bolaño, T.; Esteruelas, M. A.; Oliván, M.; Oñate, E.; Valencia, M. POP-Pincer Osmium-Polyhydrides: Head-to-Head (Z)-Dimerization of Terminal Alkynes. *Inorg. Chem.* **2013**, *52*, 6199–

6213. (b) Esteruelas, M. A.; Nolis, P.; Oliván, M.; Oñate, E.; Vallribera, A.; Vélez, A. Ammonia Borane Dehydrogenation Promoted by a Pincer-Square-Planar Rhodium(I) Monohydride: A Stepwise Hydrogen Transfer from the Substrate to the Catalyst. *Inorg. Chem.* **2016**, *55*, 7176–7181. (c) Antiñolo, A.; Esteruelas, M. A.; García-Yebra, C.; Martín, J.; Oñate, E.; Ramos, A. Reactions of an Osmium(IV)-Hydroxo Complex with Amino-Boranes: Formation of Boroxide Derivatives. *Organometallics* **2019**, *38*, 310–318. (d) Curto, S. G.; Esteruelas, M. A.; Oliván, M.; Oñate, E. Rhodium-Mediated Dehydrogenative Borylation-Hydroborylation of Bis(alkyl)alkynes: Intermediates and Mechanism. *Organometallics* **2019**, *38*, 2062–2074. (e) Esteruelas, M. A.; Oñate, E.; Paz, S.; Vélez, A. Repercussion of a 1,3-Hydrogen Shift in a Hydride-Osmium-Allenylidene Complex. *Organometallics* **2021**, *40*, 1523–1537. (f) Curto, S. G.; de las Heras, L. A.; Esteruelas, M. A.; Oliván, M.; Oñate, E.; Vélez, A. Reactions of POP-pincer rhodium(I)-aryl complexes with small molecules: coordination flexibility of the ether diphosphine. *Can. J. Chem.* **2021**, *99*, 127–136.
- (21) (a) Esteruelas, M. A.; Oliván, M.; Vélez, A. Xantphos-Type Complexes of Group 9: Rhodium versus Iridium. *Inorg. Chem.* **2013**, *52*, 5339–5349. (b) Esteruelas, M. A.; Oliván, M.; Vélez, A. POP-Pincer Silyl Complexes of Group 9: Rhodium versus Iridium. *Inorg. Chem.* **2013**, *52*, 12108–12119. (c) Alós, J.; Bolaño, T.; Esteruelas, M. A.; Oliván, M.; Oñate, E.; Valencia, M. POP-Pincer Ruthenium Complexes: d^6 Counterparts of Osmium d^4 Species. *Inorg. Chem.* **2014**, *53*, 1195–1209. (d) Alós, J.; Esteruelas, M. A.; Oliván, M.; Oñate, E.; Puylaert, P. C-H Bond Activation Reactions in Ketones and Aldehydes Promoted by POP-Pincer Osmium and Ruthenium Complexes. *Organometallics* **2015**, *34*, 4908–4921. (e) Esteruelas, M. A.; Fernández, I.; García-Yebra, C.; Martín, J.; Oñate, E. Elongated σ -Borane versus σ -Borane in Pincer-POP-Osmium Complexes. *Organometallics* **2017**, *36*, 2298–2307. (f) Esteruelas, M. A.; García-Yebra, C.; Martín, J.; Oñate, E. Dehydrogenation of Formic Acid Promoted by a Trihydride-Hydroxo-Osmium(IV) Complex: Kinetics and Mechanism. *ACS Catal.* **2018**, *8*, 11314–11323. (g) Curto, S. G.; Esteruelas, M. A.; Oliván, M.; Oñate, E.; Vélez, A. β -Borylalkenyl Z-E Isomerization in Rhodium-Mediated Diboration of Nonfunctionalized Internal Alkynes. *Organometallics* **2018**, *37*, 1970–1978. (h) Curto, S. G.; Esteruelas, M. A.; Oliván, M.; Oñate, E. Insertion of Diphenylacetylene into Rh-Hydride and Rh-Boryl Bonds: Influence of the Boryl on the Behavior of the β -Borylalkenyl Ligand. *Organometallics* **2019**, *38*, 4183–4192. (i) Esteruelas, M. A.; Fernández, I.; García-Yebra, C.; Martín, J.; Oñate, E. Cycloosmthioborane Compounds: Other Manifestations of the Hückel Aromaticity. *Inorg. Chem.* **2019**, *58*, 2265–2269. (j) Esteruelas, M. A.; Fernández, I.; Martínez, A.; Oliván, M.; Oñate, E.; Vélez, A. Iridium-Promoted B-B Bond Activation: Preparation and X-ray Diffraction Analysis of a mer-Tris(boryl) Complex. *Inorg. Chem.* **2019**, *58*, 4712–4717.
- (22) Esteruelas, M. A.; García-Yebra, C.; Martín, J.; Oñate, E. mer, fac, and Bidentate Coordination of an Alkyl-POP Ligand in the Chemistry of Nonclassical Osmium Hydrides. *Inorg. Chem.* **2017**, *56*, 676–683.
- (23) Esteruelas, M. A.; Martínez, A.; Oliván, M.; Vélez, A. A General Rhodium Catalyst for the Deuteration of Boranes and Hydrides of the Group 14 Elements. *J. Org. Chem.* **2020**, *85*, 15693–15698.
- (24) Esteruelas, M. A.; Martínez, A.; Oliván, M.; Oñate, E. Direct C-H Borylation of Arenes Catalyzed by Saturated Hydride-Boryl-Iridium-POP Complexes: Kinetic Analysis of the Elemental Steps. *Chem.—Eur. J.* **2020**, *26*, 12632–12644.
- (25) Esteruelas, M. A.; Martínez, A.; Oliván, M.; Oñate, E. Kinetic Analysis and Sequencing of Si-H and C-H Bond Activation Reactions: Direct Silylation of Arenes Catalyzed by an Iridium-Polyhydride. *J. Am. Chem. Soc.* **2020**, *142*, 19119–19131.
- (26) The structure has two chemically equivalent but crystallographically independent molecules in the asymmetric unit.
- (27) Tspis, A. C. Building trans-philicity (trans-effect/trans-influence) ladders for octahedral complexes by using an NMR probe. *Dalton Trans.* **2019**, *48*, 1814–1822.
- (28) (a) Connors, K. A. *Chemical Kinetics: The Study of Reaction Rates in Solution*; Wiley-VCH, 1990. (b) El Seoud, O. A.; Baader, W. J.; Bastos, E. L. Practical Chemical Kinetics in Solution. In *Encyclopedia of Physical Organic Chemistry*; Wang, Z., Ed.; Wiley, 2016; pp 1–68.
- (29) Luo, J.-Y. *Comprehensive Handbook of Chemical Bond Energies*; CRC Press, 2007.
- (30) For some recent examples, see: (a) Oishi, M.; Oshima, M.; Suzuki, H. A Study on Zr-Ir Multiple Bonding Active for C-H Bond Cleavage. *Inorg. Chem.* **2014**, *53*, 6634–6654. (b) Song, G.; Wang, B.; Nishiura, M.; Hou, Z. Catalytic C-H Bond Addition of Pyridines to Allenes by a Rare-Earth Catalyst. *Chem.—Eur. J.* **2015**, *21*, 8394–8398. (c) Mao, W.; Xiang, L.; Alvarez Lamsfus, C.; Maron, L.; Leng, X.; Chen, Y. Highly Reactive Scandium Phosphinoalkylidene Complex: C-H and H-H Bonds Activation. *J. Am. Chem. Soc.* **2017**, *139*, 1081–1084. (d) Kurogi, T.; Miehlisch, M. E.; Halter, D.; Mindiola, D. J. 1,2-CH Bond Activation of Pyridine across a Transient Titanium Alkylidene Radical and Re-Formation of the Ti=CH^tBu Moiety. *Organometallics* **2018**, *37*, 165–167. (e) Merz, L. S.; Wadepohl, H.; Clot, E.; Gade, L. H. Dehydrogenative coupling of 4-substituted pyridines mediated by a zirconium(II) synthon: reaction pathways and dead ends. *Chem. Sci.* **2018**, *9*, 5223–5232. (f) Zatsopin, P.; Lee, E.; Gu, J.; Gau, M. R.; Carroll, P. J.; Baik, M.-H.; Mindiola, D. J. Tebbe-like and Phosphinoalkylidene and -alkylidyne Complexes of Scandium. *J. Am. Chem. Soc.* **2020**, *142*, 10143–10152.
- (31) Esteruelas, M. A.; Forcén, E.; Oliván, M.; Oñate, E. Aromatic C-H Bond Activation of 2-Methylpyridine Promoted by an Osmium(VI) Complex: Formation of an η^2 (N,C)-Pyridyl Derivative. *Organometallics* **2008**, *27*, 6188–6192.
- (32) Beck, W.; Sünkel, K. Metal Complexes of Weakly Coordinating Anions. Precursors of Strong Cationic Organometallic Lewis Acids. *Chem. Rev.* **1988**, *88*, 1405–1421.
- (33) (a) Esteruelas, M. A.; González, A. I.; López, A. M.; Oñate, E. An Osmium-Carbene Complex with Fischer-Schrock Ambivalent Behavior. *Organometallics* **2003**, *22*, 414–425. (b) León, T.; Correa, A.; Martín, R. Ni-Catalyzed Direct Carboxylation of Benzyl Halides with CO₂. *J. Am. Chem. Soc.* **2013**, *135*, 1221–1224. (c) Ramalakshmi, R.; Maheswari, K.; Sharmila, D.; Paul, A.; Roisnel, T.; Halet, J.-F.; Ghosh, S. Reactivity of cyclopentadienyl transition metal(II)-complexes with borate ligands: structural characterization of the toluene-activated molybdenum complex [Cp*Mo(CO)₂(η^3 -CH₂C₆H₅)]. *Dalton Trans.* **2016**, *45*, 16317–16324. (d) Kelly, C. M.; Fuller, J. T., III; Macaulay, C. M.; McDonald, R.; Ferguson, M. J.; Bischof, S. M.; Sydora, O. L.; Ess, D. H.; Stradiotto, M.; Turcule, L. Dehydrogenative B-H/C(sp³)-H Benzyllic Borylation within the Coordination Sphere of Platinum(II). *Angew. Chem., Int. Ed.* **2017**, *56*, 6312–6316. (e) Espada, M. F.; Esqueda, A. C.; Campos, J.; Rubio, M.; López-Serrano, J.; Alvarez, E.; Maya, C.; Carmona, E. Cationic (η^5 -C₅Me₅Rh)^{III} Complexes with Metalated Aryl Phosphines Featuring η^4 -Phosphorus plus Pseudo-Allylic Coordination. *Organometallics* **2018**, *37*, 11–21. (f) Zamorano, A.; Rendón, N.; López-Serrano, J.; Álvarez, E.; Carmona, E. Activation of Small Molecules by the Metal-Amido Bond of Rhodium(III) and Iridium(III) (η^5 -C₅Me₅)M-Aminopyridinate Complexes. *Inorg. Chem.* **2018**, *57*, 150–162.
- (34) Lu, H.; Yu, T.-Y.; Xu, P.-F.; Wei, H. Selective Decarbonylation via Transition-Metal-Catalyzed Carbon-Carbon Bond Cleavage. *Chem. Rev.* **2021**, *121*, 365–411.
- (35) (a) Rusina, A.; Vlček, A. A. Formation of Rh(I)-Carbonyl Complex by the Reaction with Some Non-alcoholic, Oxygen-containing Solvents. *Nature* **1965**, *206*, 295–296. (b) Murakami, M.; Amii, H.; Ito, Y. Selective activation of carbon-carbon bonds next to a carbonyl group. *Nature* **1994**, *370*, 540–541. (c) Murakami, M.; Amii, H.; Shiget, K.; Ito, Y. Breaking of the C-C Bond of Cyclobutanones by Rhodium(I) and Its Extension to Catalytic Synthetic Reactions. *J. Am. Chem. Soc.* **1996**, *118*, 8285–8290. (d) Chatani, N.; Ie, Y.; Kakiuchi, F.; Murai, S. Ru₃(CO)₁₂-Catalyzed Decarbonylative Cleavage of a C-C Bond of Alkyl Phenyl Ketones. *J. Am. Chem. Soc.* **1999**, *121*, 8645–8646. (e) Daugulis, O.; Brookhart,

M. Decarbonylation of Aryl Ketones Mediated by Bulky Cyclopentadienylrhodium Bis(ethylene) Complexes. *Organometallics* **2004**, *23*, 527–534. (f) Çelenligil-Çetin, R.; Watson, L. A.; Guo, C.; Foxman, B. M.; Ozerov, O. V. Decarbonylation of Acetone and Carbonate at a Pincer-Ligated Ru Center. *Organometallics* **2005**, *24*, 186–189. (g) Lei, Z.-Q.; Li, H.; Li, Y.; Zhang, X.-S.; Chen, K.; Wang, X.; Sun, J.; Shi, Z.-J. Extrusion of CO from Aryl Ketones: Rhodium(I)-Catalyzed C-C Bond Cleavage Directed by a Pyridine Group. *Angew. Chem., Int. Ed.* **2012**, *51*, 2690–2694. (h) Whittaker, R. E.; Dong, G. Controlled Rh-Catalyzed Mono- and Double-decarbonylation of Alkynyl α -Diones To Form Conjugated Ynones and Disubstituted Alkynes. *Org. Lett.* **2015**, *17*, 5504–5507. (i) Somerville, R. J.; Martin, R. Forging C-C Bonds Through Decarbonylation of Aryl Ketones. *Angew. Chem., Int. Ed.* **2017**, *56*, 6708–6710. (j) Morioka, T.; Nishizawa, A.; Furukawa, T.; Tobisu, M.; Chatani, N. Nickel-Mediated Decarbonylation of Simple Unstrained Ketones through the Cleavage of Carbon-Carbon Bonds. *J. Am. Chem. Soc.* **2017**, *139*, 1416–1419. (k) Sarju, J. P.; Dey, D.; Torroba, J.; Whitwood, A. C.; Redeker, K.; Bruce, D. W. Catalytic Activation of Unstrained, Nonactivated Ketones Mediated by Platinum(II): Multiple C-C Bond Cleavage and CO Extrusion. *Organometallics* **2019**, *38*, 4539–4542.

(36) Gyton, M. R.; Kynman, A. E.; Leforestier, B.; Gallo, A.; Lewandowski, J. R.; Chaplin, A. B. Isolation and structural characterisation of rhodium(III) η^2 -fluoroarene complexes: experimental verification of predicted regioselectivity. *Dalton Trans.* **2020**, *49*, 5791–5793.

(37) Jawad, J. K.; Puddephatt, R. J.; Stalteri, M. A. Selectivity in Reactions of Alkyl-Aryl-Transition-Metal Complexes with Electrophiles. *Inorg. Chem.* **1982**, *21*, 332–337.

(38) Peña-López, M.; Ayán-Varela, M.; Sarandeses, L. A.; Pérez Sestelo, J. Palladium-Catalyzed Cross-Coupling Reactions of Organogold(I) Reagents with Organic Electrophiles. *Chem.—Eur. J.* **2010**, *16*, 9905–9909.